Redox Biology 74 (2024) 103238

Contents lists available at ScienceDirect

Redox Biology

journal homepage: www.elsevier.com/locate/redox

Manganese porphyrin-based treatment improves fetal-placental development and protects against oxidative damage and NLRP3 inflammasome activation in a rat maternal hypothyroidism model

Jeane Martinha dos Anjos Cordeiro [a], Luciano Cardoso Santos [a], Bianca Reis Santos [a], Acácia Eduarda de Jesus Nascimento [a], Emilly Oliveira Santos [a], Erikles Macêdo Barbosa [a], Isabela Oliveira de Macêdo [a], Letícia Dias Mendonça [a], José Ferreira Sarmento-Neto [b], Clarice Santos Pinho [c], Erick Teixeira dos Santos Coura [c], Acácio de Sá Santos [a], Marciel Elio Rodrigues [d], Júlio Santos Rebouças [b], Gilson De-Freitas-Silva [c], Alexandre Dias Munhoz [a], Mário Sérgio Lima de Lavor [a], Juneo Freitas Silva [a,*]

[a] Centro de Microscopia Eletrônica, Departamento de Ciências Biológicas, Universidade Estadual de Santa Cruz, Ilhéus, Brazil
[b] Departamento de Química, Centro de Ciências Exatas e da Natureza, Universidade Federal da Paraíba, Joao Pessoa, Brazil
[c] Departamento de Química, Instituto de Ciências Exatas, Universidade Federal de Minas Gerais, Belo Horizonte, Brazil
[d] Departamento de Ciências Exatas e Tecnológicas, Universidade Estadual Do Sudoeste da Bahia, Vitória da Conquista, Brazil

ARTICLE INFO

Keywords:
Thyroid
Metalloporphyrin
Antioxidant
Placenta
Inflammasome
Rat

ABSTRACT

Oxidative stress (OS) and endoplasmic reticulum stress (ERS) are at the genesis of placental disorders observed in preeclampsia, intrauterine growth restriction, and maternal hypothyroidism. In this regard, cationic manganese porphyrins (MnPs) comprise potent redox-active therapeutics of high antioxidant and anti-inflammatory potential, which have not been evaluated in metabolic gestational diseases yet. This study evaluated the therapeutic potential of two MnPs, $[MnTE\text{-}2\text{-}PyP]^{5+}$ (MnP I) and [MnT(5-Br-3-E-Py)P]5+ (MnP II), in the fetal-placental dysfunction of hypothyroid rats. Hypothyroidism was induced by administration of 6-Propyl-2-thiouracil (PTU) and treatment with MnPs I and II 0.1 mg/kg/day started on the 8th day of gestation (DG). The fetal and placental development, and protein and/or mRNA expression of antioxidant mediators (SOD1, CAT, GPx1), hypoxia (HIF1α), oxidative damage (8-OHdG, MDA), ERS (GRP78 and CHOP), immunological (TNFα, IL-6, IL-10, IL-1β, IL-18, NLRP3, Caspase1, Gasdermin D) and angiogenic (VEGF) were evaluated in the placenta and decidua on the 18th DG using immunohistochemistry and qPCR. ROS and peroxynitrite (PRX) were quantified by fluorometric assay, while enzyme activities of SOD, GST, and catalase were evaluated by colorimetric assay. MnPs I and II increased fetal body mass in hypothyroid rats, and MnP I increased fetal organ mass. MnPs restored the junctional zone morphology in hypothyroid rats and increased placental vascularization. MnPs blocked the increase of OS and ERS mediators caused by hypothyroidism, showing similar levels of expression of HIFα, 8-OHdG, MDA, *Gpx1*, GRP78, and *Chop* to the control. Moreover, MnPs I and/or II increased the protein expression of SOD1, Cat, and GPx1 and restored the expression of IL10, *Nlrp3*, and *Caspase1* in the decidua and/or placenta. However, MnPs did not restore the low placental enzyme activity of SOD, CAT, and GST caused by hypothyroidism, while increased the decidual and placental protein expression of TNFα. The results show that treatment with MnPs improves the fetal-placental development and the placental inflammatory state of hypothyroid rats and protects against oxidative stress and reticular stress caused by hypothyroidism at the maternal-fetal interface.

* Corresponding author. Centro de Microscopia Eletrônica, Departamento de Ciências Biológicas, Universidade Estadual de Santa Cruz, Campus Soane Nazaré de Andrade, 45662Rodovia Jorge Amado, km 16, Salobrinho, Ilhéus, Bahia, Brazil.
E-mail address: jfsilva@uesc.br (J.F. Silva).

https://doi.org/10.1016/j.redox.2024.103238
Received 26 March 2024; Received in revised form 7 June 2024; Accepted 9 June 2024
Available online 11 June 2024

1. Introduction

Gestational diseases such as preeclampsia, intrauterine growth restriction, recurrent miscarriage, and gestational diabetes mellitus are associated with oxidative stress and endoplasmic reticulum (reticular) stress at the maternal-fetal interface [1–7]. Maternal hypothyroidism is another important gestational disease that affects from 2.5 % to 15 % of pregnant women, depending on the region and case notifications effectiveness [8–10]. Recently, we demonstrated that this disease also causes oxidative and reticular stress at the maternal-fetal interface of rats, with dysregulation of the expression and reduced activity of antioxidant enzymes and increased mediators of reticular stress [11].

Studies have already shown that hypothyroidism increases the frequency of miscarriages [12,13]. It is also reportedly associated with the occurrence of preeclampsia [14,15] and causes premature neonates with lower body mass and congenital anomalies [16,17]. In addition, in rats, maternal hypothyroidism resulted in failures in intrauterine trophoblastic migration and apoptosis, and reduced trophoblastic proliferation and expression of angiogenic and immunological mediators such as interleukin 10 (IL-10), inducible nitric oxide synthase 2 (NOS2), vascular endothelial growth factor (VEGF), and placental growth factor (PIGF) in the maternal-fetal interface [18–20].

Thyroid hormones are important regulators of oxygen and antioxidant consumption in the body [21,22]. Moreover, thyroid hypofunction compromises antioxidant activity and lipid metabolism [23,24]. Therefore, the use of synthetic or natural antioxidants in the treatment of placental dysfunction caused by maternal hypothyroidism may be promising. These antioxidants can also prevent other gestational diseases that involve oxidative and reticular stress in their pathogenesis, such as preeclampsia and recurrent miscarriage [25,26]. In this regard, in recent years, studies have shown that cationic water-soluble manganese porphyrins (MnPs) of the *N*-alkylpyridylporphyrin class have excellent therapeutic potential in the control of oxidative stress (redox modulators) as redox-active therapeutics in models of stroke, renal ischemia, and radioprotection because of their high antioxidant power, minimal toxicity, and high bioavailability associated with their lipophilicity [27,28].

MnPs are versatile compounds since the porphyrin ring can be altered to obtain compounds with tailored properties. Some examples of metalloporphyrins of use as redox-active therapeutics are [MnTE-2-PyP]$^{5+}$, [MnTM-2-PyP]$^{5+}$, [MnT*n*Bu-2-PyP]$^{5+}$, [MnT*n*Hex-2-PyP]$^{5+}$, and [MnT*n*BuOE-2-PyP]$^{5+}$ [29–33]. [MnTE-2-PyP]$^{5+}$, *meso*-tetrakis (*N*-ethylpyridinium-2-yl)porphyrinatomanganese(III), and *meso*-tetrakis (*N*-(2′-*n*-butoxyethyl)pyridinium-2-yl)porphyrinatomanganese(III) ([MnT*n*BuOE-2-PyP]$^{5+}$) are in Phase II clinical trial studies for atopic dermatitis and pruritus ([MnTE-2-PyP]$^{5+}$), and for glioma, head and neck cancer ([MnT*n*BuOE-2-PyP]$^{5+}$) [34–37]. These metalloporphyrins can regulate transcription factors such as hypoxia-inducible factor 1 alpha (HIF1α) and nuclear factor kappa B (NF-κB), which are redox-dependent, as well as suppress inflammatory processes mediated by oxidative stress [38,39]. In addition, MnPs have anti-inflammatory action by affecting the immune responses of T helper lymphocytes 1 (Th1) and 2 (Th2), thus reducing cytokines such as interferon gamma (IFNy) and interleukins 4 (IL-4) and 5 (IL-5) [40]. However, to date, no study has been conducted with MnPs for the treatment of metabolic gestational diseases that occur with placental stress.

Since hypothyroidism causes oxidative stress and reticular stress in the maternal-fetal interface of rats [11], the hypothesis of this study is that MnPs may prevent or reduce fetal and placental changes caused by maternal hypothyroidism. Thus, the aim was to evaluate the therapeutic potential of two formulations of MnPs, [MnTE-2-PyP]$^{5+}$ and [MnT(5-Br-3-E-Py)P]5+, *meso*-tetrakis-(5-bromo-3-*N*-ethylpyridinium)porphyrinatomanganese(III), in the fetal and placental restriction of rats with hypothyroidism. The findings showed that the two MnPs evaluated, one of which is [MnT(5-Br-3-E-Py)P]5+ and not yet described in the literature, were able to improve fetal development and placental morphology and vascularization of rats with hypothyroidism. This effect was associated with reduced oxidative and reticular stress, increased expression of antioxidant enzymes, and reduced HIF1α, IL10, *Nlrp3*, and *Caspase 1* expression at the maternal-fetal interface.

2. Material and methods

2.1. Synthesis and characterization of manganese porphyrins (MnPs)

[MnTE-2-PyP]Cl_5, *meso*-tetrakis(*N*-ethylpyridinium-2-yl)porphyrinatomanganese(III) chloride, specified as [MnTE-2-PyP]$^{5+}$ in aqueous solution, was prepared and purified as previously reported [41] and showed chromatographic and spectroscopic characterizations consistent with published data [42–44]. For this work, aqueous stock solutions of [MnTE-2-PyP]$^{5+}$ were prepared and their concentrations in 1 mM range were determined spectrophotometrically using published molar absorptivity value ($\varepsilon_{454.0\ nm}$ = 138,038 cm^{-1} M^{-1}) [41].

[MnT(5-Br-3-E-Py)P]Cl_5, *meso*-tetrakis(5-bromo-*N*-ethylpyridinium-3-yl)porphyrinatomanga-nese(III) chloride, a new metalloporphyrin specified in aqueous solutions as [MnT(5-Br-3-E-Py)P]5+, was prepared in three steps, using an adaptation of literature procedures [41,45]. In the first step, the free base porphyrin H_2T(5-Br-3-Py)P was obtained as follows: 28.1 mL of acetic acid was heated to 90 °C, then 2.16 g of 5-bromo-3-pyridinecarboxaldehyde (113 mmol, ALDRICH) and 0.8 mL pyrrole (113 mmol, freshly distilled, ALDRICH) were added. The system was left under reflux for 60 min. After this time, the system was cooled to room temperature (25 °C). Then, a solution of sodium acetate trihydrate (0.73 M) was added to the reaction mixture, until an approximate pH 3. The precipitate formed was filtered under vacuum and washed with hot water. The solid was collected with a mixture of chloroform and methanol (2:1). Purification was performed by column chromatography, using alumina as the stationary phase, and a mixture of chloroform: methanol as the mobile phase in the following proportions: 100:1, 50:1, 30:1, 2:1, and 1:1. Fractions corresponding to H_2T(5-Br-3-Py)P were combined and the solvent was removed on a rotary evaporator. H_2T(5-Br-3-Py)P was characterized by UV–Vis electronic absorption spectroscopy and hydrogen nuclear magnetic resonance (^{1}H NMR).

In the second step, the free base porphyrin H_2T(5-Br-3-E-Py)PCl_4, specified as H_2T(5-Br-3-E-Py)P^{4+} in aqueous solution, was synthesized by alkylation of the precursor H_2T(5-Br-3-Py)P using an adaptation of a literature procedure [41]. H_2T(5-Br-3-Py)P (150 mg, 0.16 mmol) and ethyl tosylate (6 mL, 6.9 g, 34.5 mmol) were dissolved in *N*,*N*-dimethylformamide (30 mL) and heated to 110 °C under magnetic stirring for 24h. The alkylation reaction was monitored by thin layer chromatography, using H_2O:KNO_3(aq):MeCN 1:1:8 (v/v/v) as eluent, and UV–Vis electronic absorption spectroscopy as reported for the free base analog H_2TE-2-PyP^{4+} [41]. The resulting H_2T(5-Br-3-E)PyP^{4+} sample was isolated and purified as the chloride salt, H_2T(5-Br-3-E)$PyPCl_4$, as described previously [41]. H_2T(5-Br-3-E)$PyPCl_4$ was characterized by UV–Vis absorption spectroscopy.

In the third step, H_2T(5-Br-3-E)$PyPCl_4$ was metallated with manganese. In a beaker, 94.92 mg (796 μmol) of H_2T(5-Br-3-E)$PyPCl_4$ was solubilized in 30 mL of water, keeping the system under magnetic stirring. Then, 1 mol L^{-1} sodium hydroxide solution was added, drop by drop, until pH 12. Subsequently, 271.35 mg (1.37 mmol) of manganese (II) chloride tetrahydrate, previously solubilized in a minimal amount of water, was added. The system was kept under agitation for 5 min until reaching pH 8. The metalation reaction was monitored by UV–Vis electronic absorption spectroscopy. The resulting [MnT(5-Br-3-E-Py)P]$^{5+}$ sample was isolated and purified as the chloride salt ([MnT(5-Br-3-E-Py)P]Cl_5) as described previously [41]. The product was characterized by UV–Vis electronic absorption spectroscopy ($\varepsilon_{461.0\ nm}$ = 140,920 cm^{-1} M^{-1}) and mass spectrometry (ESI-MS).

2.2. Experimental design

Adult Wistar rats (230–250g) were used in this study. The females were fed with commercial rat chow (NUVILAB ® Cr-1, Nuvital, Colombo, PR, Brazil) and water *ad libitum* and kept under controlled brightness (12 h of light/12 h of dark) and temperature (22 °C). All procedures were approved by the Ethics Committee on the Use of Animals of the *Universidade Estadual de Santa Cruz* (Protocol No. 002/17).

After 7 days of adaptation, the rats were randomly separated into groups control, MnP I, and MnP II (experiment 1), and the groups control, hypothyroid, hypo + MnP I, and hypo + MnP II (experiment 2). Each group consisted of 6–7 animals.

The first experiment was carried out to verify if the administration of MnPs could compromise fetal-placental development since, until now, they had never been used during pregnancy in rats. The estrous cycle of the rats was monitored daily, and after checking two complete estrous cycles (proestrus, estrus, diestrus), the rats in proestrus were placed with adult male rats (1 female/1 male) for 12h overnight. The next morning, vaginal smears were performed, and copulations were confirmed by the presence of sperm in the vaginal cytology. That day was designated as day 0 of gestation. Treatment with MnPs was daily (see dosing and administration details below), starting on the 8th DG, and euthanasia occurred on the 18th DG. The entire genital system was collected, as well as the liver, spleen, lungs, heart, brain, and kidneys for histopathological evaluation. Blood was collected for plasma analyses of biomarkers of liver, kidney, and heart function.

In experiment 2, the animals received 6-Propyl-2-thiouracil (PTU; 4 mg/kg/day) in distilled water through an orogastric tube to induce hypothyroidism [19]. Three days after the start of induction, the females of all groups underwent vaginal cytology and the rats in proestrus were kept with adult male rats (1 female/1 male) for 12h overnight. Copulations were confirmed the next morning by the presence of sperm in the vaginal cytology (0 DG). The rats that tested positive for pregnancy were kept separate according to the experimental group. Euthanasia was performed on 18th DG. The placental discs were collected for histomorphometry analysis of the placenta, analysis of protein and gene expression by immunohistochemistry and real-time polymerase chain reaction (qPCR), and evaluation of antioxidant enzyme activity, ROS and peroxynitrite levels.

2.3. Administration of manganese porphyrins (MnPs)

For experiment 1, the groups treated with MnPs were formed by the group MnP I ([MnTE-2-PyP]5+ and the group MnP II ([MnT(5-Br-3-E-Py)P]5+. In experiment 2, the groups hypothyroid (PTU) + MnP I and hypothyroid (PTU) + MnP II were formed. MnP I has antioxidant activity (ROS and RNS modulation) already described in other diseases [42], but has not yet been evaluated in metabolic gestational diseases. It was used as a reference to evaluate MnP II, a new metalloporphyrin without *in vitro* and *in vivo* studies to determine its antioxidant activity and therapeutic potential. Treatment with MnPs was daily, from the 8th to the 18th DG. The treatment was initiated in the post-implantation period and the beginning of placentation [46] to eliminate the possibility of the drug affecting embryo implantation. The drugs were diluted in sterile physiological solution and administered at a dosage of 0.1 mg/kg/day, intraperitoneally (IP) [31]. The control group (sham) received the same volume of sterile physiological solution (300 μL), intraperitoneally.

2.4. Necropsy and material collection

The rats were euthanized with a guillotine and 5 mL of blood was collected in heparin tubes to obtain plasma. The blood was centrifuged at 3000 rpm for 20 min and the plasma obtained was stored at −20 °C.

In experiments 1 and 2, the uteri containing the placentas and fetuses were separated from the fallopian tubes and ovaries. Subsequently, the uteri containing placentas and fetuses, uteri with placentas without fetuses, and all fetuses were individually weighed. An estimate of the amniotic fluid mass was also obtained after subtracting the mass of the uterus and placenta with the fetuses from the mass of the fetuses and the mass of the uterus and placenta without the fetuses. The number of fetuses and the number of sites with fetal resorption or death were also counted. Then, in experiment 2, placental discs were randomly removed from both horns of each group. Two placental discs were removed, dissected, and separated from the decidua. One of the discs was packed in a microtube, immediately frozen in liquid nitrogen, and then stored at −80 °C to evaluate antioxidant enzyme activity and dosage of reactive oxygen species (ROS) and peroxynitrite (PRX, a representative RNS). The other placental disc was stored in a microtube containing TRIzol, immediately frozen in liquid nitrogen, and stored at −80 °C for subsequent qPCR. The remaining discs, as well as the maternal organs collected in experiment 1, were fixed in 4 % paraformaldehyde at 4 °C for 24h and processed through the paraffin embedding technique. The tissues were dehydrated in solutions with increasing concentrations of alcohol (70 %–100 %), with subsequent diaphanization in xylol and paraffin impregnation and embedding. Histological sections 4 μm thick of tissues were obtained by microtomy on histological slides and stained with hematoxylin and eosin for histopathological and histomorphometry analyses. Silane-coated polarized slides (StarFrost Polycat, Germany) were used for immunohistochemistry.

2.5. Evaluation of plasma biochemistry and free T3 and T4 profile

In experiment 1, plasma levels of alanine aminotransferase (ALT), aspartate aminotransferase (AST), alkaline phosphatase (ALP), total proteins, albumin, urea, creatinine, and creatine kinase on 18th DG were analyzed using commercial colorimetric kits.

In experiment 2, the dosage of free T3 and T4 on 18th DG was performed by enzyme-linked immunosorbent assay (ELISA) (sensitivity: 0.4 NG/dL), with commercial kits and according to the manufacturer's instructions (IMMULITE, Siemens Medical Solutions Diagnostics, Malvern, PA, USA). The intra- and inter-assay coefficients of variation were 4 % and 7 %, respectively.

2.6. Assessment of fetal development

The heart, liver, lungs, and kidneys of each fetus were dissected and weighed. To analyze fetal body mass distribution and risk of fetal growth restriction, fetal body mass histograms were constructed for each group with individual fetal mass, followed by nonlinear regression performed according to Dilworth et al. (2011). The 5th percentile was calculated as: (-Z score × SD) + mean, assuming that Z score = 1.645, SD = standard deviation, mean = mean of the control group.

2.7. Histomorphometry analysis of the placenta

The histomorphometry analysis was performed on 6–7 placental discs/group. Histological sections were performed in the center of the placental disc to include the central maternal blood vessel, thus ensuring the histological sections were uniform. Images of each placental disc were captured using a Leica S9i stereomicroscope. The thickness of each layer of the placenta [junctional zone (JZ) and placental labyrinth (PL)] was evaluated in 10 random regions and a mean was obtained for each placental disc. The analysis was carried out using Image Pro Plus software version 4.5 and the values were transformed to millimeters.

In the JZ, the proportion of area occupied by glycogen cells, spongiotrophoblasts, and trophoblastic giant cells was evaluated in five random fields at 200 × magnification. The average of the five random fields represented the proportion of cellular components of the JZ of each placenta. In the PL, the proportion of area occupied by maternal vascular sinus, fetal capillaries, and fetal mesenchyme/trophoblast cells was evaluated in 10 random fields at 400 × magnification. The average

of the 10 random fields represented the proportion of tissue components of the PL of each placenta. The images were captured in a Leica DM2500 photon microscope and the quantification was performed in graticule of 99 (JZ) and 100 (PL) points using Image Pro Plus software version 4.5 [47,48].

2.8. Immunohistochemistry (IHC)

Histological sections of the placenta with decidua basalis and the metrial gland were submitted to immunohistochemistry analysis. The antibodies used were anti-HIF1α (1:1000, sc-13515), anti-8-OHdG (1:200, sc-393871), anti-SOD1 (1:1000, sc-365858), ant-GPx1/2 (1:1000, sc-133160), anti-catalase (1:1000, SC-271803), anti-GRP78 (1:1000, SC - 13539), anti-CHOP (1:1000, SC-71136), anti-VEGF (1:200, SC-152), anti-TNFα (1:500, SC-52746), anti-IL-10 (1:6000, SC-365858), all from Santa Cruz Biotechnology, CA, USA, and anti-MDA (1:1000, ab243066; ABCAM, Cambridge, UK).

The streptavidin-biotin-peroxidase technique was used by the Dako detection system (EnVision™ FLEX+, Mouse, High pH, (Link)) and antigenic recovery was performed by heated water bath at 98 °C using citric acid solution (0.54 M; pH 6.0). The sections were immersed for 30 min in a hydrogen peroxide solution (3 %; H_2O_2) in methanol (CH_3OH) to block endogenous peroxidase, then kept for another 30 min in a blocking serum solution (Ultra vision Block, Lab Vision Corp., Fremont, CA. USA), followed by incubation with the primary antibodies in a humidity chamber overnight. Incubation with secondary antibody conjugated to streptavidin peroxidase (EnVision™ FLEX/HRP; ref. SM802) occurred for 30 min. The chromogen used was 3′3 diaminobenzidine (EnVision™ FLEX DAB + Chromogen; ref. DM827), diluted in buffer with H_2O_2 (EnVision™ FLEX Substrate Buffer; 1:50; ref. SM803). Lastly, the sections were counterstained with Harris hematoxylin. The negative control was obtained by replacing the primary antibody with phosphate buffered solution (PBS) or normal mouse IgG (1:200; sc-2025, Santa Cruz Biotechnology, CA, USA) [19,49].

Descriptive and quantitative evaluations were conducted of the immunostaining of HIF1α, 8-OHdG, MDA, SOD1, catalase, GPx1/2, GRP78, CHOP, VEGF, IL-10, and TNFα in the decidua (decidua basalis + metrial triangle), JZ and PL of the maternal-fetal interface. The quantitative evaluation was performed randomly in six placental discs/group with images of five random fields of each evaluated region. The images were obtained with a Leica DMI 300B photon microscope (Leica Microsystems, Germany) at 400 × magnification. For this evaluation, the WCIF ImageJ® software (Media Cybernetics Manufacturing, Rockville, MD, USA) was used. Color deconvolution and thresholding images were taken. The data of each tissue were archived, analyzed, and expressed as immunostaining area in pixels [19].

2.9. Real-time PCR (qPCR)

To perform the qPCR, mRNA was first extracted from the placenta using TRIzol (Invitrogen, Life Technologies, Carlsbad, CA, USA), according to the manufacturer's protocol. cDNA synthesis was performed with 1 μg of RNA using the SuperScript III First-Strand Synthesis SuperMix Kit (Invitrogen). Gene transcripts of target genes were quantified by qPCR using PowerUp™ SYBR™ Green (Master Mix Applied Biosystems™ PowerUp™ SYBR™ Green, Thermo Fisher Scientific) on the Applied Biosystems 7500 Fast Real-time PCR System (Applied Biosystems, Life Technologies). For qPCR reactions, 1 μL of cDNA, 100 nM of each primer, and 7.5 μL of PowerUp reagent were used in a final volume of 15 μL of reaction. In the negative control, the DNA amplification mix was used, in which the cDNA sample was replaced by water. The amplifications were performed under the following conditions: enzyme activation at 95 °C for 10 min, 40 cycles of denaturation at 95 °C for 15 s, and annealing/extension at 60 °C for 60 s. A qPCR amplification efficiency test was performed using serial dilutions of cDNA, together with an evaluation of the qPCR melting curve of the amplification products. The primers were designed based on the mRNA sequence of *Rattus norvegicus* (Table 1). Gene expression was analyzed by the $2^{-\Delta\Delta CT}$ method, in which the results obtained for each group were compared quantitatively after normalization based on the expression of RNA *polymerase II subunit A* (*Polr2a*) of *Rattus norvegicus* [11,50].

2.10. Evaluation of enzyme activity of superoxide dismutase (SOD), glutathione S-transferase (GST), and catalase

The placental samples were homogenized in potassium phosphate buffer (TFK) (50 mM; pH 7.0) and centrifuged at 13,400 rpm for 10 min at 4 °C to collect supernatants. The protein concentration was evaluated by the method of [51], while the enzyme activities of SOD, GST, and catalase were evaluated according to Refs. [52–54], respectively.

2.11. Evaluation of placental ROS and peroxynitrite levels

The ROS and peroxynitrite (PRX) in placental discs were quantified by fluorometric assay with specific probes for ROS (2′,7′-dichlorofluorescein diacetate; DCFH-DA, Invitrogen, Life Technologies, Carlsbad, CA, USA) and peroxynitrite (dihydrorhodamine 123, Invitrogen, Life Technologies, Carlsbad, CA, USA) [11,55]. Fluorescence was measured with a fluorometer (Synergy 2 SL Luminescence Microplate Reader; Biotek) using excitation and emission wavelengths of 500 nm. Data were expressed as arbitrary units (AU) of fluorescence + SEM. These tests were conducted in duplicate.

2.12. Statistical analysis

The data are presented as mean ± standard error of the mean (SEM) and were tested for normality (Shapiro-Wilk) and homoscedasticity (Brown-Forsythe) of the residues. Analysis of variance (ANOVA) was

Table 1
List of genes and nucleotide sequences for qPCR primers.

Gene	Sequence (5->3)	Accession number
Hif1a	F: AGCAATTCTCCAAGCCCTCC R: TTCATCAGTGGTGGCAGTTG	NM_024359.1
Nrf2	F: CCCATTGAGGGCTGTGATCT R: GCCTTCAGTGTGCTTCTGGTT	NM_031789.2
Sod1	F: GAAAGGACGGTGTGGCCAAT R: CTCGTGGACCACCATAGTACG	NM_017050.1
Gpx1	F: GCGCTACAGCGGATTTTTGA R: GAAGGCATACACGGTGGACT	NM_030826.3
Cat	F: CTGACTGACGCGATTGCCTA R: GTGGTCAGGACATCGGGTTT	NM_012520.2
Grp78	F: TGAAGGGGAGCGTCTGATTG R: TCATTCCAAGTGCGTCCGAT	NM_013083.2
Chop	F: TGGCACAGCTTGCTGAAGAG R: TCAGGCGCTCGATTTCCT	NM_001109986.1
Vegf	F: GCCCAGACGGGGTGGAGAGT R: AGGGTTGGCCAGGCTGGGAA	NM_001110336.1
Tnf	F: AGCCCGTAGCCCACGTCGTA R: CGGTGTGGGTGAGGAGCACG	NM_012675.3
Il6	F: GACTTCCAGCCAGTTGCCTT R: AAGTCTCCTCTCCGGACTTGT	NM_053595.2
Il10	F: GGCCATTCCATCCGGGGTGA R: AAGGCAGCCCTCAGCTCTCG	NM_012854.2
Nlrp3	F: CTCTGCATGCCGTATCTGGT R: GTCCTGAGCCATGGAAGCAA	NM_001191642.1
Caspase1	F: ACAAAGAAGGTGGCGCATTT R: GTGCTGCAGATAATGAGGGC	NM_012762.2
Il1β	F: GCACAGTTCCCCAACTGGTA R: TGTCCCGACCATTGCTGTTT	NM_031512.2
Il18	F: ACCACTTTGGCAGACTTCACT R: ACACAGGCGGGTTTCTTTTG	NM_019165.1
Gasdermin d	F: AAGATCGTGGATCATGCCGT R: AAGATCGTGGATCATGCCGT	NM_001130553.1
Polr2a	F: GCTGGACCTACTGGCATGTT R: ACCATAGGCTGGAGTTGCAC	NM_001079162.5

performed followed by the Student-Newman-Keuls test (SNK). Generalized linear analysis of mixed models followed by Tukey's test were used to assess fetal body mass [56]. The analyses were performed using GraphPad Prism 8.0.2® software and the differences were considered significant when $P < 0.05$.

A Principal Component Analysis (PCA) was conducted for each dataset to link the variables used with the groups assessed in each treatment. Initially, the variables related to the evaluated groups were standardized using the *decostand function* (*method* = "*standardize*") to enhance data accuracy. Subsequently, a data imputation process was carried out using the *imputePCA function* to address missing data (*NA*) [57,58]. Finally, the relationship between the most correlated variables (>0.60) and their association with the groups within each treatment was examined [59]. All analyses were performed in Program R, version 4.3.3, utilizing the *vegan*, *missMDA, FactoMineR*, and *factoextra packages*.

3. Results

3.1. Preparation of metalloporphyrins [MnTE-2-PyP]$^{5+}$and [MnT(5-Br-3-E-Py)P]5+

The metalloporphyrin [MnTE-2-PyP]$^{5+}$ was prepared and purified as previously reported [41] and the resulting spectroscopic and chromatographic characterizations were consistent with published data [42–44].

The novel metalloporphyrin [MnT(5-Br-3-E-Py)P]5+ was obtained in three steps, as shown in Supplementary Fig. 1. In the first step, neutral free base H_2T(5-Br-3-Py)P was obtained with a yield of 8.5 % (339 mg) and showed a UV–Vis absorption spectrum (Supplementary Fig. 2), which is typical of a free base porphyrin, with a Soret band at 419 nm and four Q bands in the visible region originating from $\pi \rightarrow \pi^*$ transitions [60]. The ^{1}H NMR spectrum (Supplementary Fig. 3) showed all the characteristic signals of the porphyrin macrocycle, including the signal at $\delta = -2.90$ ppm, characteristic of the hydrogen atom attached to each pyrrole nitrogen atom, shielded by the porphyrin π-current.

In the second step, the water-soluble derivative H_2T(5-Br-3-E-Py)P^{4+} was obtained in 90 % yield and showed UV–Vis absorption spectra typical of free base porphyrins [60]. In the last step, the metalloporphyrin of interest, [MnT(5-Br-3-E-Py)P]5+, was obtained with 85 % yield. The UV–Vis spectrum of [MnT(5-Br-3-E-Py)P]5+ (Supplementary Fig. 2) was consistent with the spectra of other manganese described in the literature [61]. Comparison of the UV–Vis spectra of free bases porphyrins (H_2T(5-Br-3-Py)P and H_2T(5-Br-3-E-Py)P^{4+}) and [MnT(5-Br-3-E-Py)P]5+ revealed changes in the spectral profile consistent with the metalation reaction. The metalation with manganese resulted in a red shift of Soret band (from ~420 nm in the free base to 461 nm in MnP). Also, the number of free-base Q bands were reduced in MnP, which is consistent with an increase of the macrocycle local symmetry from D_{2h} (free base) to D_{4h} (MnP). Strong interaction between the orbitals of the porphyrin macrocycle and the orbitals of the metal could account for these changes [61]. Mass spectrometry analysis was conducted using the ESI-MS technique. For [MnT(5-Br-3-E-Py)P]5+ (Supplementary Fig. 4), the most intense peaks were observed at 242.22, 284.28, 390.79, and 604.98. These peaks correspond to [MnT(5-Br-3-E-Py)P + $6H_2O$]$^{5+}$, [MnT(5-Br-3-E-Py)P + Cl^-]$^{4+}$, [MnT(5-Br-3-E-Py)P + 2 Cl^-]$^{3+}$, and [MnT(5-Br-3-E-Py)P + 3 Cl^-]$^{2+}$ respectively. Similar fragmentation patterns shown in Supplementary Fig. 4 were observed for other cationic *N*-alkylpyridylporphyrins [62,63].

3.2. The administration of MnPs during pregnancy did not compromise the plasma biochemistry and fetal and placental development of Wistar rats

First, we verified whether the administration of metalloporphyrins [MnTE-2-PyP]$^{5+}$ (MnP I) and [MnT(5-Br-3-E-Py)P]$^{5+}$ (MnP II) could compromise the pregnancy of Wistar rats since these drugs had not been used during pregnancy in experimental rat models. According to the results, MnPs at a dose of 0.1 mg/kg/day from the 8th DG did not affect plasma levels of ALT, AST, ALP, total proteins, albumin, urea, and creatinine compared to control ($P > 0.05$), while MnP I reduced plasma levels of creatine kinase (Supplementary Table 1; $P < 0.05$). The administration of MnPs did not affect the mass of the uterus + placental unit and amniotic fluid (Supplementary Figs. 5A–B) or the histology of maternal organs (heart, liver, lungs, kidneys, brain, and spleen) (Supplementary Fig. 6). Moreover, the use of MnPs did not affect the number of fetuses and did not compromise fetal body mass on 18th DG (Supplementary Figs. 5C–D; $P < 0.05$).

3.3. MnPs improves the fetal body mass and placental morphology of hypothyroid rats

In the first experiment, the administration of MnPs did not compromise plasma biochemistry, the histology of the maternal organs, and the reproductive parameters of Wistar rats. Therefore, the therapeutic potential of these MnPs in the fetal and placental restriction in rats with hypothyroidism [19,47] was evaluated in the second experiment. Initially, the induction and maintenance of hypothyroid status in rats treated with PTU was confirmed since the plasma levels of free T3 and T4 on 18th DG in this group were lower than the control (Fig. 1A and B; $P < 0.0001$) and treatment with MnPs did not alter the profile of these hormones.

According to the evaluation of maternal and placental parameters, MnP I and MnP II were not able to increase the lower uteroplacental and amniotic fluid mass observed in the hypothyroid rats when compared to the control (Fig. 1C and D; $P < 0.05$; $P < 0.01$). In addition, no significant difference was observed in the number of fetuses in relation to the hypothyroid group, which were reduced compared to the control group (Fig. 1E; $P < 0.05$). However, MnPs were able to increase the low fetal body mass observed in the hypothyroid rats (Fig. 1F; $P < 0.05$; $P < 0.01$). The relative frequency of fetal body mass distribution showed that the distribution of 96.84 % of the fetuses of the control animals was higher than the 5th percentile (1.280 g). In contrast, the body mass of only 5.31 % of the fetuses of the hypothyroid group was higher than the 5th percentile, with deviation to the left of the relative distribution curve (Fig. 1G). The fetal body mass of the animals treated with MnPs I and II was, respectively, 22.39 % and 22.36 % above the 5th percentile, suggesting improved fetal development. Interestingly, treatment with MnP I also increased the organ mass (liver, kidneys, heart, lungs) of the fetuses of hypothyroid rats, which were reduced compared to the control (Fig. 1H; $P < 0.0001$).

Since treatment with MnPs improved the fetal development of hypothyroid rats, we verified whether this effect could be associated with a change in placental morphology, as no difference was observed in the mass of the uterus-placenta unit. According to the results, MnPs partially restored the thickness of the PL of the hypothyroid rats since hypothyroidism reduced the thickness of this layer in relation to the control and the treatment with the MnPs did not differ significantly in relation to the control (Fig. 2A and B). Furthermore, MnPs I and II restored the cellularity of the JZ since hypothyroidism increased the proportion of glycogen cells in this layer of the placenta (Fig. 2C; $P < 0.01$) and MnPs reduced this population, matching the control (Fig. 2C; $P > 0.05$). In the PL, MnPs not only increased the area occupied by maternal vascular sinus compared to the control (Fig. 2D; $P < 0.05$; $P < 0.01$), as also increased the area occupied by fetal capillary compared to the control and hypothyroid groups (Fig. 2D; $P < 0.001$; $P < 0.0001$), which was reduced in the hypothyroid group compared to the control ($P < 0.05$). Regarding the area occupied by fetal mesenchyme/trophoblast, a reduction was observed in the MnPs groups compared to the control and hypothyroid groups (Fig. 2D; $P < 0.01$ $P < 0.001$; $P < 0.0001$).

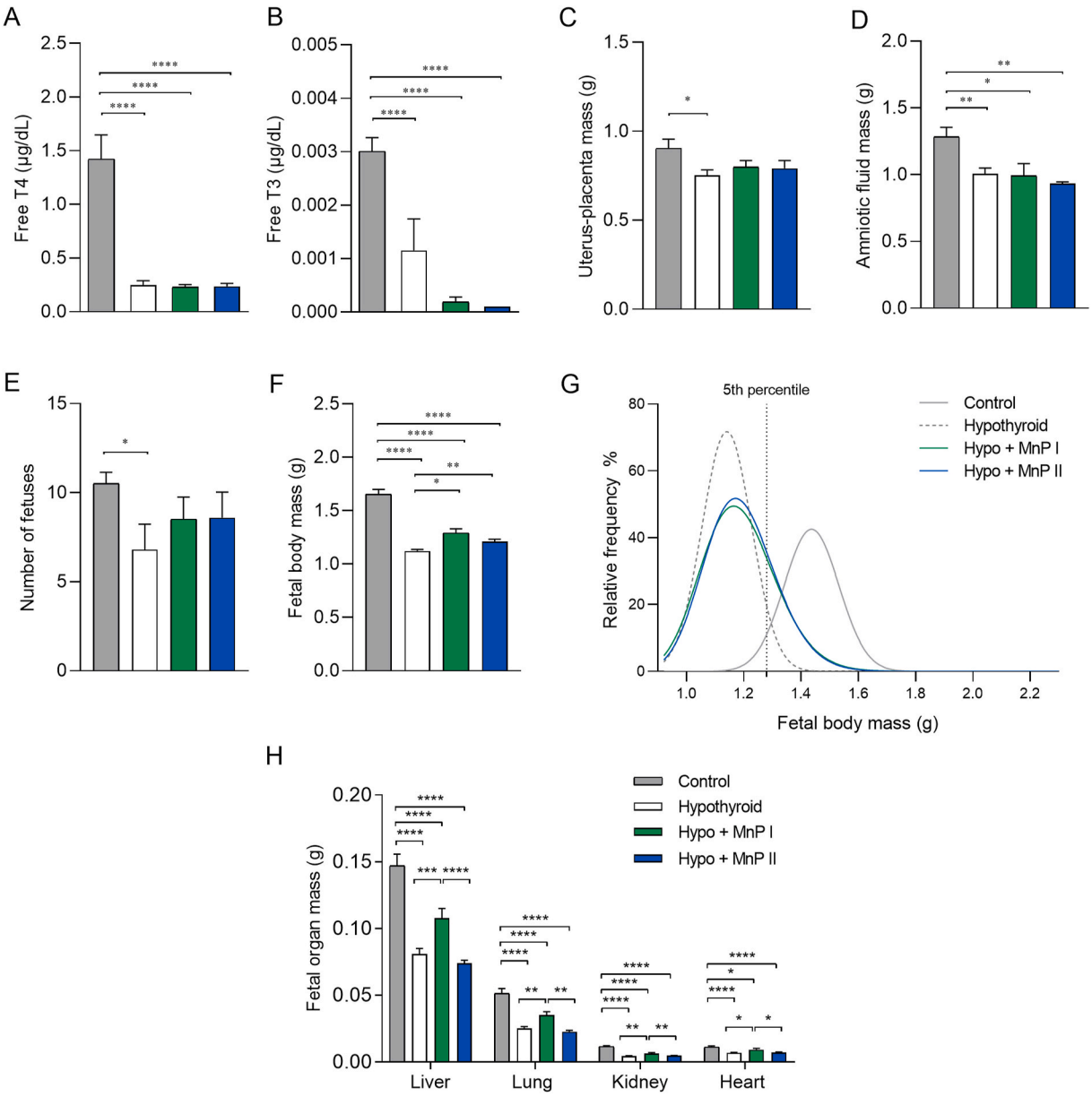

Fig. 1. Plasma levels of free T3 and T4 and reproductive parameters of control, hypothyroid, and hypothyroid rats treated with $[MnTE\text{-}2\text{-}PyP]^{5+}$ (MnP I) and $[MnT(5\text{-}Br\text{-}3\text{-}E\text{-}Py)P]^{5+}$ (MnP II). A) Free T4. B) Free T3. C) Uterus and placental mass; D) Amniotic fluid mass; E) Number of fetuses; F) Fetal body mass; G) Relative frequency of fetal body mass distribution. H) Fetal liver, kidney, heart, and lung mass (mean ± SEM; *P < 0.05; **P < 0.01; ***P < 0.001; *P < 0.0001; SNK test (A–E); Generalized linear analysis of mixed models followed by Tukey test (F); N = 5–7/group (A–E); N = 22–31/group (F); N = 19–31/group (H)).

3.4. MnPs reduces HIF1α expression at the maternal-fetal interface of hypothyroid rats

Treatment with MnPs improved placental morphology and fetal development of hypothyroid rats. Moreover, recent studies have suggested that hypoxia occurs in the maternal-fetal interface of rats with hypothyroidism [11]. Therefore, we evaluated the expression of HIF1α, a marker of hypoxia [64], and of *Nrf2*, a transcription factor involved in the expression of antioxidant enzymes [65]. Immunostaining of HIF1α at the maternal-fetal interface of the animals demonstrated that MnPs I and II reduced the protein expression of HIF1α in the decidua and JZ of hypothyroid rats (Fig. 3A and B; $P < 0.05$; $P < 0.01$), matching the expression of the control rats ($P > 0.05$). This is consistent with treatment with Mn(III) *N*-alkylpyridylporphyrins downregulating HIF1α in other experimental animal models [39,66]. Although the literature effects of MnPs on transcription factors are usually evaluated by immunohistochemistry, we complimented this analysis by evaluating also the gene expression. The same result as that of immunohistochemistry was obtained for gene expression, in which treatment with MnP I reduced mRNA expression for *Hif1α* in the placenta of hypothyroid rats (Fig. 3C; $P < 0.05$), matching the control ($P > 0.05$). Regarding the expression of transcripts for *Nrf2,* although hypothyroidism increased its placental expression in relation to the control ($P < 0.05$), treatment with MnPs did not show a significant difference regarding the hypothyroid and control groups (Fig. 3C; $P > 0.05$).

3.5. MnPs blocks the increase of 8-OHdG and MDA at the maternal-fetal interface of hypothyroid rats

Since MnPs reduced HIF1α expression at the maternal-fetal interface of hypothyroid rats, we evaluated the immunostaining of 8-hydroxy-2′-deoxyguanosine (8-OHdG) and malondialdehyde (MDA), biomarkers of

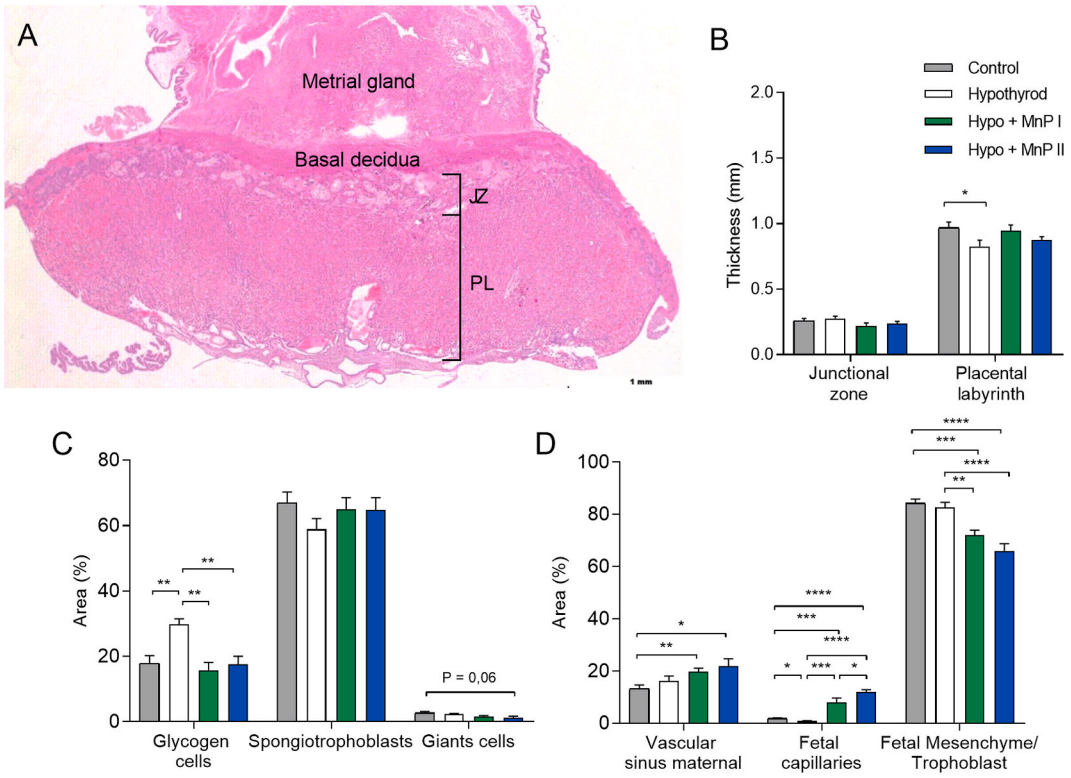

Fig. 2. Histomorphometry analysis of the placenta of control, hypothyroid, and hypothyroid rats treated with [MnTE-2-PyP]$^{5+}$ (MnP I) and [MnT(5-Br-3-E-Py)P]$^{5+}$ (MnP II). A) Photomicrography of the maternal-fetal interface showing the decidua and placenta on 18th DG (hematoxylin and eosin staining; Bar = 500 μm) B) Thickness of the JZ (giant cells + spongiotrophoblast) and PL; C) Percentage of area occupied by glycogen cells, spongiotrophoblasts, and giant cells in the JZ (mean ± SEM; *P < 0.05; **P < 0.01; SNK test; N = 0.01; 6–8/group); D) Percentage of area occupied by maternal vascular sinus, fetal capillary, and fetal mesenchyme/trophoblast of the PL (mean ± SEM; *P < 0.05; **P < 0.01; ***P < 0.001; ****P < 0.0001; * * * *P < 0.0001; SNK test; n = 6–8/group). JZ = Junctional zone; LP = Placental labyrinth.

oxidative DNA damage and lipid peroxidation, respectively [67,68]. Interestingly, treatment with MnPs I and II blocked the higher decidual expression of 8-OHdG and MDA observed in the hypothyroid group (Fig. 4A–D; P < 0.001; P < 0.0001), matching the expression of the control group (P > 0.05), as well as the higher MDA expression in the PL caused by maternal hypothyroidism (Fig. 4D; P < 0.01).

3.6. MnPs increases the protein expression of antioxidant enzymes at the maternal-fetal interface of hypothyroid rats and restores placental gene expression of Gpx1

The expression of HIF1α, 8-OHdG, MDA, and *Nrf2* increased in the maternal-fetal interface of the hypothyroid group, while treatment with MnPs reduced the expression of HIF1α, 8-OHdG, and MDA. Therefore, we evaluated the expression and/or enzyme activity of SOD1, catalase, GPx1, and GST, the main antioxidant enzymes involved in the control of oxidative stress under hypoxic conditions [69,70], as well as the placental levels of ROS and peroxynitrite. Immunohistochemistry analysis demonstrated that treatment with MnPs I and II increased SOD1 immunostaining in the JZ and PL in relation to the control and hypothyroid groups and in the decidua compared to the control rats (Fig. 5A and B; P < 0.05; P < 0.01). In contrast, MnP I reduced the placental expression of transcripts for *Sod1* in relation to the hypothyroid group (Fig. 5G; P < 0.05).

The immunostaining of GPx1/2, like SOD1, also increased in the JZ and PL by the treatment with the MnPs in relation to the control and hypothyroid groups (Fig. 5C and D; P < 0.01). Regarding gene expression, both treatments also restored the mRNA expression of *Gpx1*, with reduced levels relative to the hypothyroid group and matching the control (Fig. 5G).

Regarding the immunostaining of catalase, an increase in expression was observed in the decidua and JZ of hypothyroid rats treated with MnP II in relation to the other groups, and in the PL in relation to the hypothyroid group (Fig. 5E–F, P < 0.05; P < 0.001). In the gene expression analysis, treatment with MnPs I and II did not alter the higher expression of *Cat* observed in the hypothyroid rats in relation to the control (Fig. 5G). Of note, this class of MnPs are not mimics of catalase [71]. Regarding the enzyme activity of SOD, catalase, and GST in the placenta, treatment with MnPs did not alter the lower activity caused by hypothyroidism in relation to the control (Fig. 5H; P < 0.01; P < 0.001; P < 0.0001). Moreover, no differences were observed in the placental levels of ROS and peroxynitrite between the groups (Fig. 5I; P > 0.05).

3.7. MnPs reduces the expression of endoplasmic reticulum stress mediators at the maternal-fetal interface of hypothyroid rats

Because we demonstrated that hypothyroidism causes endoplasmic reticulum stress in the maternal-fetal interface of rats [11], we verified whether treatment with MnPs I and II could also reverse this process. For this purpose, we analyzed the expression of GRP78 and CHOP, which are key mediators of the activation pathway of unfolded protein response (UPR) and indicate the occurrence of reticular stress [72–74]. MnPs I and II reversed the higher decidual expression of GRP78 caused by hypothyroidism (Fig. 6A and B; P < 0.01), matching the expression of the control group (P > 0.05). No difference was observed in *Grp78* gene expression between the groups (Fig. 6E).

Regarding CHOP immunostaining, MnP I reduced the higher decidual expression caused by hypothyroidism, while both MnPs did not alter the higher expression in the JZ observed in hypothyroid rats compared to the control (Fig. 6C and D). Interestingly, MnP I and II

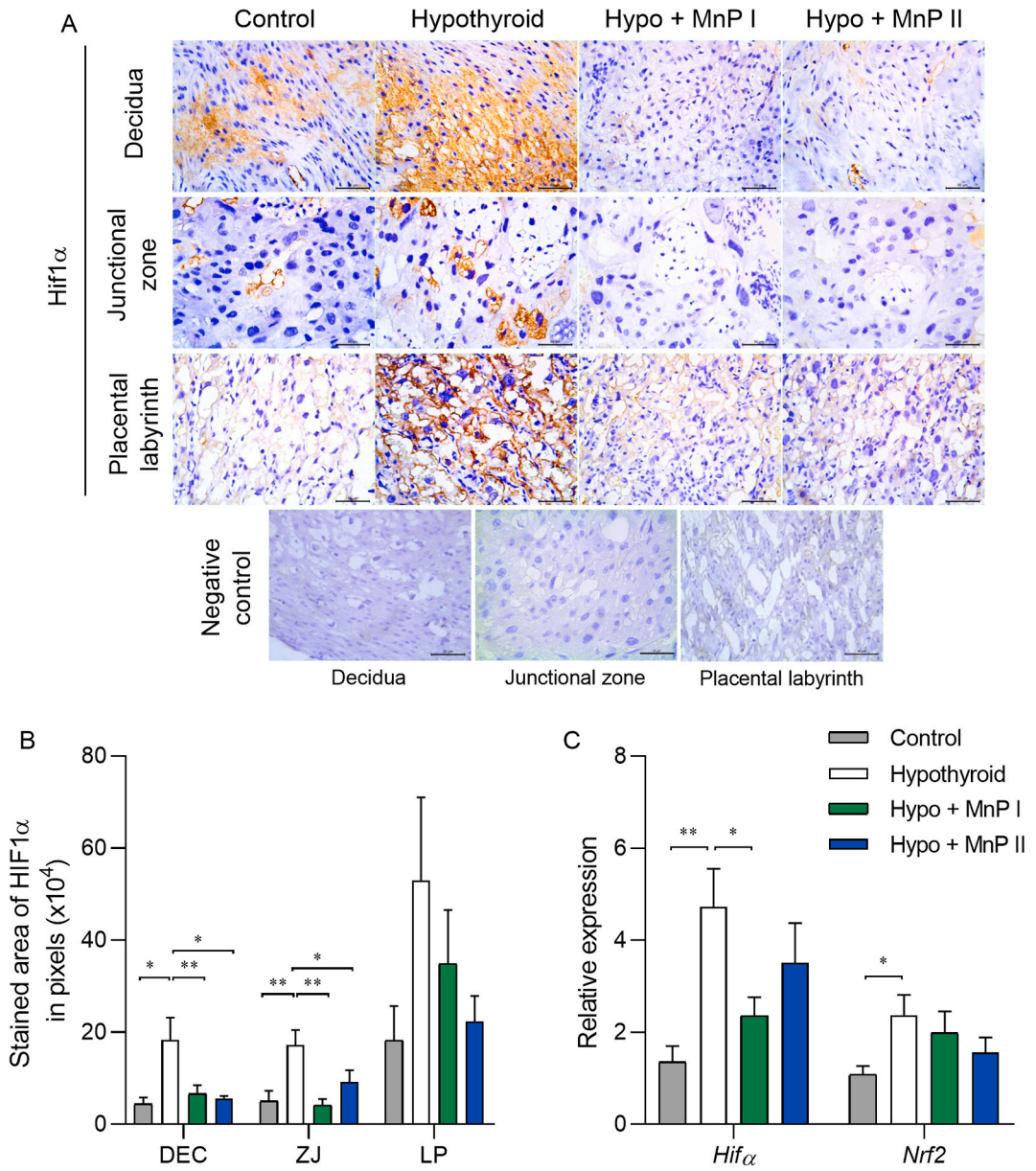

Fig. 3. Expression of HIF1α and *Nrf2* at the maternal-fetal interface of control, hypothyroid, and hypothyroid rats treated with $[MnTE\text{-}2\text{-}PyP]^{5+}$ (MnP I) and $[MnT(5\text{-}Br\text{-}3\text{-}E\text{-}Py)P]^{5+}$ (MnP II). A) Photomicrographs of HIF1α immunolabeling in the decidua, junctional zone, placental labyrinth, and negative control (streptavidin-biotin-peroxidase, contrasted with Harris hematoxylin, Bar = 50 μm). B) Immunostaining area in pixels of HIF1α in the decidua, junctional zone, and placental labyrinth; C) Relative gene expression of *Hif1α and Nrf2* in the placenta (mean ± SEM, *P < 0.05; **P < 0.01; SNK test; N = 6–8/group).

increased CHOP expression in the PL of hypothyroid rats (Fig. 6D; P < 0.05; P < 0.01). In contrast, both porphyrins reduced the higher placental gene expression of *Chop* caused by hypothyroidism (Fig. 6E; P < 0.01), matching the control (P > 0.05).

3.8. MnP I reduces VEGF expression at the placental junctional zone of hypothyroid rats

The protein expression of VEGF in the maternal-fetal interface of these animals was also evaluated since it is important angiogenic mediator for adequate placental function [46], in addition to being an indicator of hypoxia by signaling via HIF1α [75]. MnP I reduced the higher VEGF immunostaining in the JZ caused by hypothyroidism (Fig. 7A and B; P < 0.05), matching the control (P > 0.05), while no differences were observed when rats were treated with MnP II. In the PL and decidua, the higher VEGF expression caused by hypothyroidism was not altered by treatment with MnPs (Fig. 7B). There was no significant difference in placental *Vegf* gene expression between groups (Fig. 7C; P > 0.05).

3.9. MnPs restores IL10 expression and reduces Nlrp3 and Caspase 1 expression at the maternal-fetal interface of hypothyroid rats

Since oxidative and reticular stress favors the increase of inflammatory cytokines [76,77] and hypothyroidism in rats causes NLRP3 inflammasome activation and pyroptosis at the maternal-fetal interface [78], we evaluated the expression of important pro- (TNFα and IL-6) and anti-inflammatory (IL-10) cytokines, in addition to the gene expression of mediators of the NLRP3 inflammasome via (*Nlrp3*, *Caspase1*, *Il1β*, *Il18*) and pyroptosis (*Gasdermin d*).

Regarding TNFα, MnPs I and II increased their expression in the PL and decidua, respectively, in relation to the control and hypothyroid

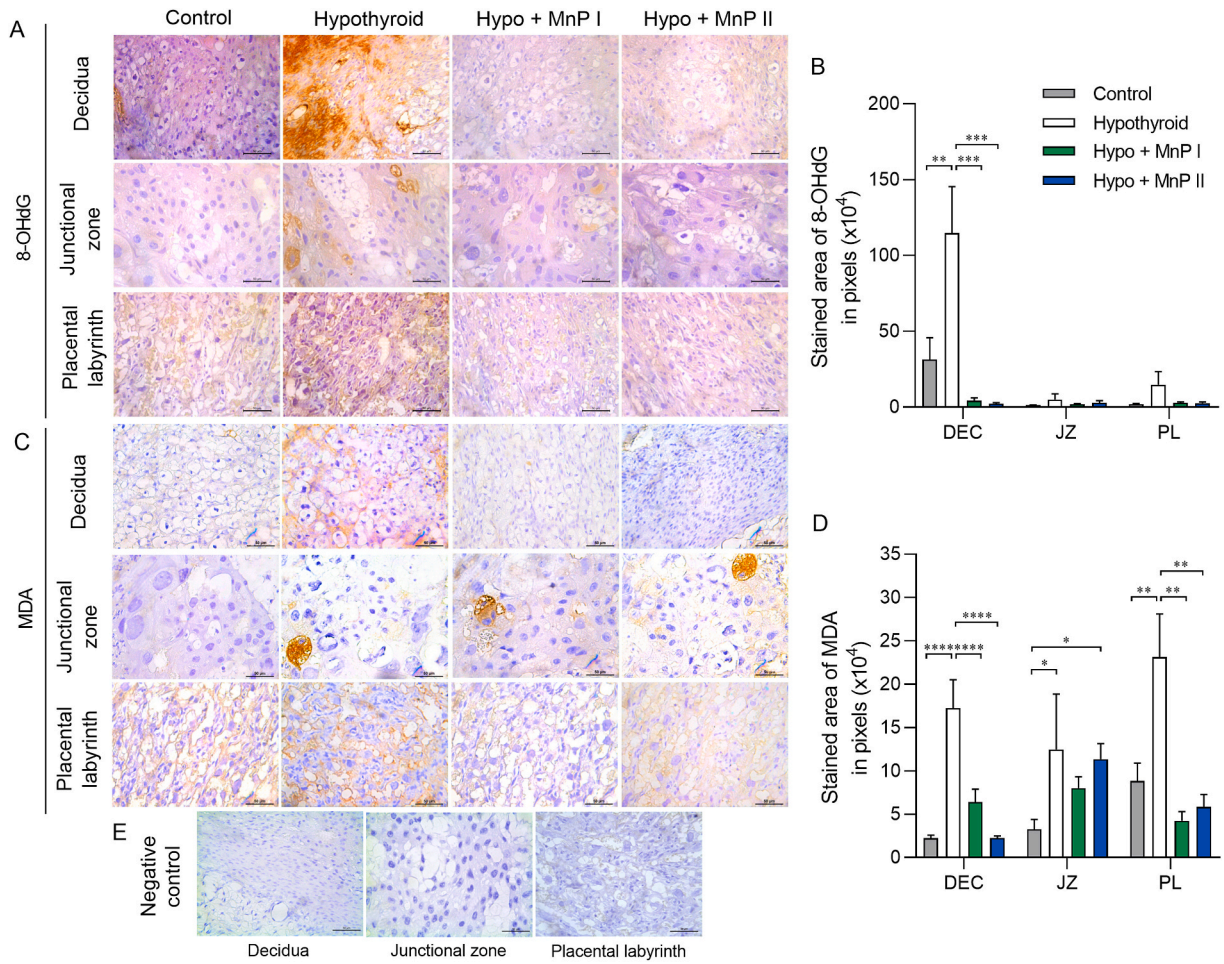

Fig. 4. Expression of 8-OHdG and MDA in the decidua and placenta of control, hypothyroid, and hypothyroid rats treated with [MnTE-2-PyP]$^{5+}$ (MnP I) and [MnT(5-Br-3-E-Py)P]$^{5+}$ (MnP II). A and C) Photomicrographs of the immunostaining of 8-OHdG (A) and MDA (C) in the decidua, junctional zone, and placental labyrinth (streptavidin-biotin-peroxidase, contrasted with Harris hematoxylin, Bar = 50 μm). B and D) Immunostaining area in pixels of 8-OHdG (B) and MDA (D) in the decidua, junctional zone, and placental labyrinth. E) Negative Control (mean ± SEM, **P < 0.01; ***P < 0.001; SNK test; N = 6–7/group).

groups (Fig. 8A and B; P < 0.01; P < 0.001; P < 0.0001). In the JZ, the MnPs did not alter the higher TNFα expression caused by hypothyroidism (Fig. 8B). However, MnP I reduced placental gene expression of *Tnf* compared to the hypothyroid group (Fig. 8E; P < 0.05). Regarding *Il6*, there was no difference in gene expression between the groups (Fig. 8E; P > 0.05).

In relation to IL-10, interestingly, both metalloporphyrins reduced the higher decidual expression caused by hypothyroidism, matching the control group (Fig. 8C and D). In the PL, MnP I also reduced IL-10 immunostaining in hypothyroid rats (P < 0.01), matching the control. In the JZ, no significant difference was observed in IL-10 immunostaining between the groups (Fig. 8D; P > 0.05). Regarding *Il10* gene expression, MnPs also reduced the higher placental expression caused by hypothyroidism, matching the control group (Fig. 8E; P > 0.05).

When evaluating the genes involved in the NLRP3 inflammasome activation, MnPs reversed the higher gene expression of *Nlrp3* caused by hypothyroidism (Fig. 8F; P < 0.01), matching the control (P > 0.05), while MnP I also reduced the higher placental expression of *Caspase1* caused by hypothyroidism (Fig. 8E; P < 0.05). There was no significant difference in the expression of *Il1β* and *Il18* between the groups, while MnPs were also not able to reduce the higher placental expression of *Gasdermin d* observed in hypothyroid rats (Fig. 8F).

3.10. PCA analysis

PCA analyses were carried out on both placental and fetal development data, antioxidant activity data, data on protein expression in JZ, PL, and decidua, and placental gene expression data.

Regarding placental development data, the cumulative contribution of the axes accounted for 73.4 % of the data (PC1: 49.7 %; PC2: 23.7 %). Among the variables positively correlated with the PC1 axis, we observed the fetal mesenchyme and trophoblast, primarily associated with the control group; and the amniotic fluid, more closely linked to the control and Hypo + MnP I groups. The PC2 axis showed a positive correlation with the glycogen cells, which were linked to the hypothyroid group (Fig. 9A and Supplementary Table 2). In terms of fetal development data, the cumulative contribution of the axes explained 87 % of the data (PC1: 73.7 %; PC2: 13.3 %). The Heart, Liver, Lung, Kidney, and Body Mass were strongly associated with the control and Hypo + MnP I groups (Fig. 9A and Supplementary Table 2), indicating a more favorable impact of MnP I on fetal development compared to MnP II.

For antioxidant activity data and protein expression in JZ, the cumulative explained variance of the axes was 65.4 % (PC1: 48.3 % and PC2: 17.1 %). Among the variables positively associated with PC1, VEGF was linked to the Hypo + MnP II group, while SOD, CAT, and CHOP were mainly related to the Hypo + MnP I and Hypo + MnP II groups. PC2 showed a positive correlation with GPX, predominantly encompassing the Hypo + MnP I group (Fig. 9C and Supplementary Table 2). With respect to the protein expression data in PL, the total explained variance of the axes was 77.3 % (PC1: 45 % and PC2: 32.3 %). SOD, CHOP, and VEGF were positively correlated with PC1, relatively

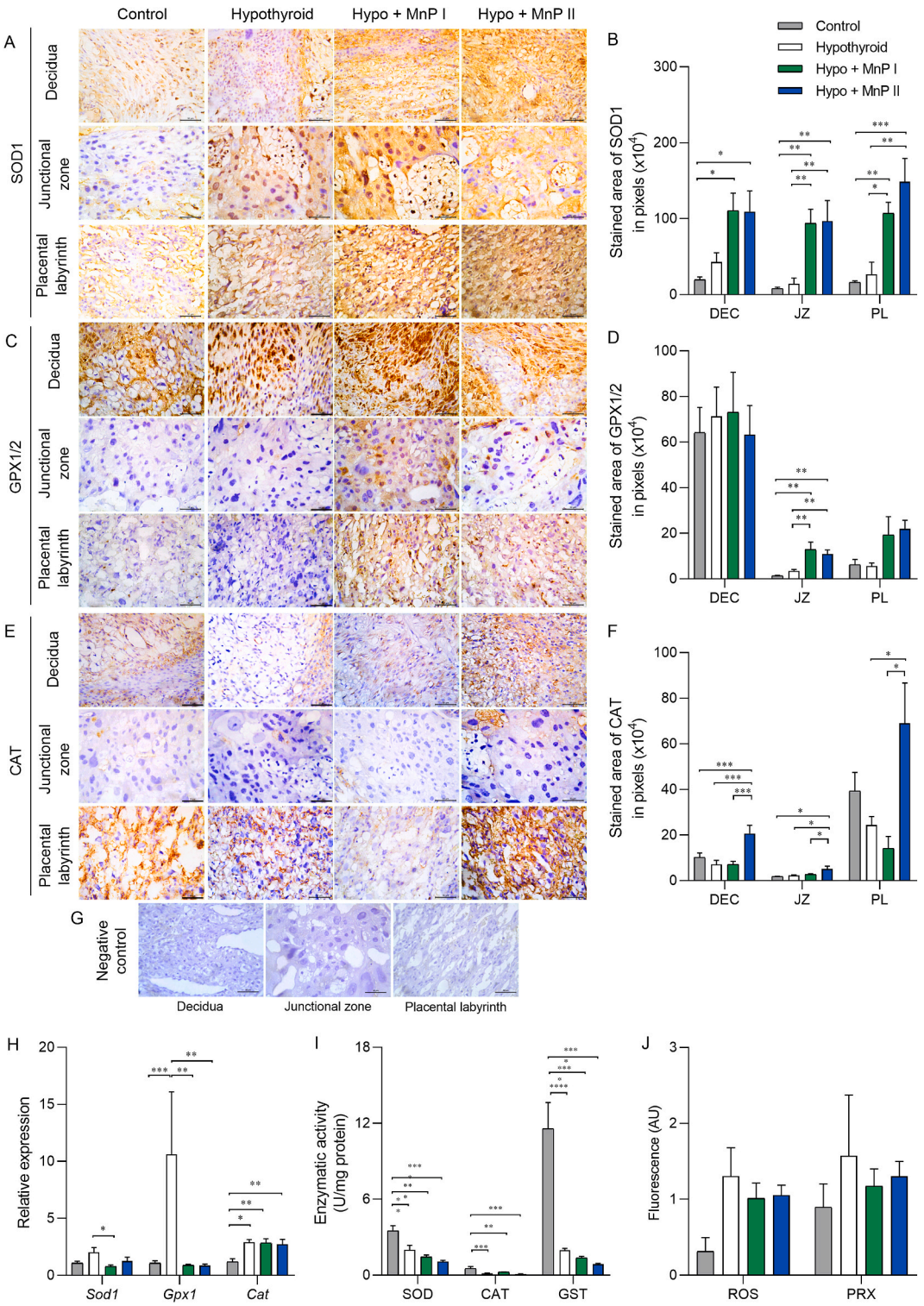

Fig. 5. Expression and activity of antioxidant enzymes and plasma levels of ROS and peroxynitrite at the maternal-fetal interface of control, hypothyroid, and hypothyroid rats treated with [MnTE-2-PyP]$^{5+}$ (MnP I) and [MnT(5-Br-3-E-Py)P]$^{5+}$ (MnP II). A, C, E) Photomicrographs of the immunostaining of SOD1 (A), GPx1 (C), and catalase (E) in the decidua, junctional zone, and placental labyrinth (streptavidin-biotin-peroxidase, contrasted with Harris hematoxylin, Bar = 50 μm). B, D, F) Immunostaining area in pixels of SOD1 (B), GPx1 (D), and catalase (F) in the decidua, junctional zone, and placental labyrinth. G) Negative Control. H) Relative gene expression of *Sod1*, *Gpx1,* and *Cat* in the placenta. I) Enzyme activity of SOD, catalase, and GST in the placenta. J) Placental levels of ROS and peroxynitrite (PRX) (mean ± SEM, *P < 0.05; **P < 0.01; ***P < 0.001; ****P < 0.0001; SNK test; N = 6–8/group).

associated with the two Mn porphyrins (MnP I and MnP II). In PC2, there were positive correlations involving IL10, associated with both Mn porphyrins and the hypothyroid group; and MDA, strongly linked to the hypothyroid group (Fig. 9D and Supplementary Table 2).

For the protein expression data in the decidua, the cumulative explained variance of the axes was 67.8 % (PC1: 38.9 % and PC2: 28.9 %). Variables positively correlated with PC1 were strongly linked to the hypothyroid group, including 8-OhdG, HIF 1α, IL10, MDA, and GRP78.

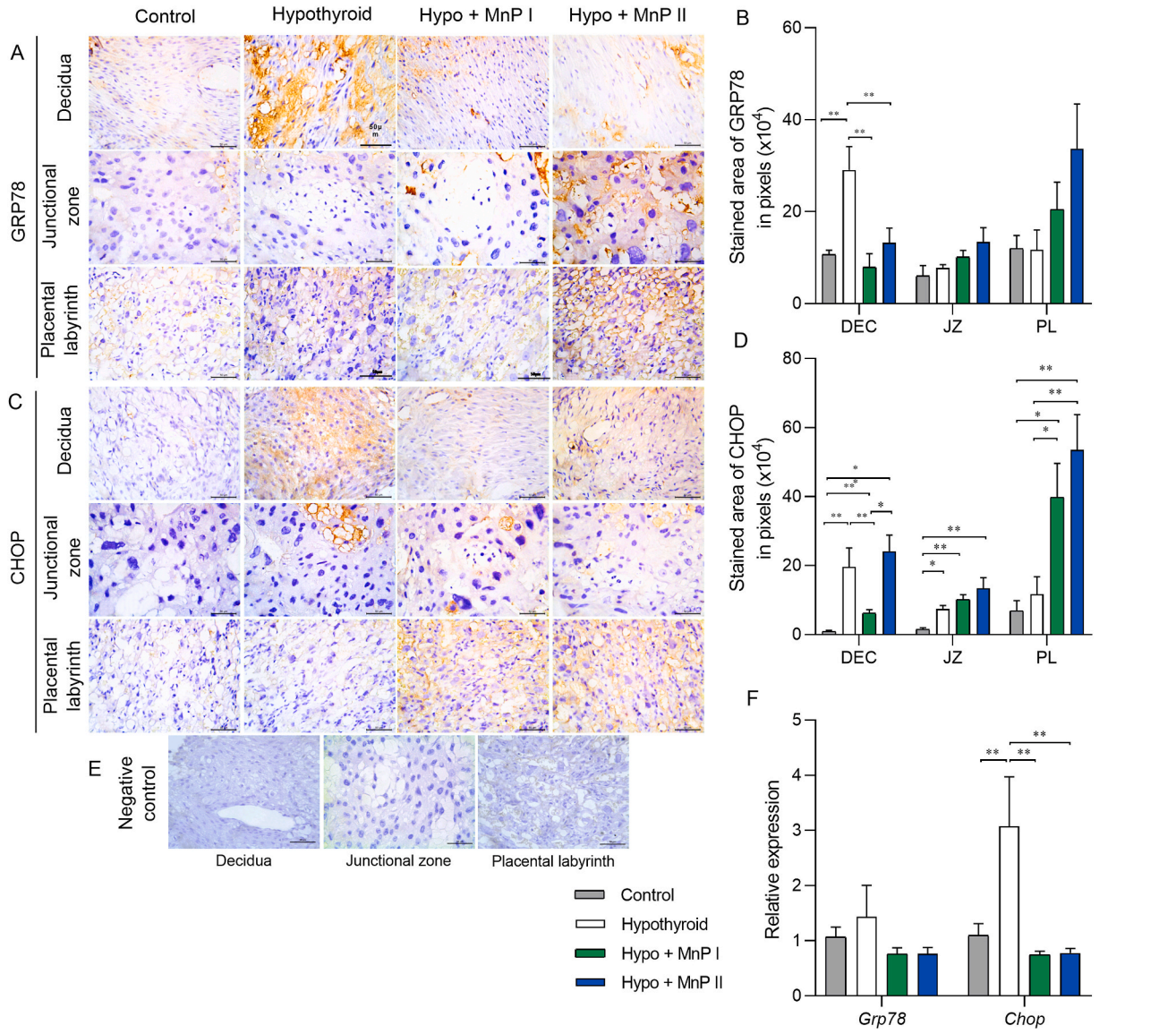

Fig. 6. Expression of GRP78 and CHOP at the maternal-fetal interface of control, hypothyroid, and hypothyroid rats treated with [MnTE-2-PyP]$^{5+}$ (MnP I) and [MnT(5-Br-3-E-Py)P]$^{5+}$ (MnP II). A-C) Photomicrographs of the immunostaining of GRP78 (A) and CHOP (C) in the decidua, junctional zone, and placental labyrinth (streptavidin-biotin-peroxidase, contrasted with Harris hematoxylin, Bar = 50 μm). B-D) Immunostaining area in pixels of GRP78 (B) and CHOP (D) in the decidua, junctional zone, and placental labyrinth; E) Negative Control. F) Relative gene expression of *Grp78 and Chop* in the placenta (mean ± SEM, *P < 0.05; **P < 0.01; SNK test; N = 6–8/group).

Conversely, CAT showed a negative correlation with PC1 and was closely associated with the Hypo + MnP II group. PC2 included variables that were positively correlated and predominantly associated with MnP I and MnP II (VEGF, SOD, CHOP, and TNFα) (Fig. 9E and Supplementary Table 2). In terms of gene expression data, the total explained variance of the axes was 63.3 % (PC1: 42.5 % and PC2: 20.8 %). Variables exhibiting a positive correlation with PC1 were linked to the hypothyroid group, such as *Sod1*, *Hif1α*, *Il10*, *Chop*, and *Nlrp3*. For PC2, *Gasdd* and *Casp1* were positively correlated and displayed a stronger association with the hypothyroid and Hypo + MnP II groups (Fig. 9F and Supplementary Table 2).

Overall, PCA analysis revealed a significant link between hypothyroidism and the presence of mediators of hypoxia, oxidative stress, reticular stress, and inflammasome activation at the maternal-fetal interface. Both MnPs were found to reduce the expression of these factors, particularly MnP I, which showed a more positive impact on fetal development.

4. Discussion

This study demonstrated that the administration of MnPs improves the fetal development and placental morphology and vascularization of rats with maternal hypothyroidism. Furthermore, it was found that MnPs provided protection against oxidative stress and endoplasmic reticulum stress at the maternal-fetal interface of these animals and restored the placental and/or decidual expression of IL-10, while reduced gene expression of mediators of the inflammasome-NLRP3 via. This is the first study to evaluate the therapeutic potential of MnPs in a metabolic gestational disease associated with placental stress and assess [MnT(5-Br-3-E-Py)P]5+ in an experimental model of disease.

Since MnPs I and II had not been used in a metabolic gestational disease, we initially sought to verify the safety of their administration during pregnancy in Wistar rats. Both MnPs I and II did not compromise the number of fetuses, fetal body mass, mass of the uterus + placental unit, and amniotic fluid. In addition, the administration of MnPs did not affect the histology of the maternal organs, including the histology of the

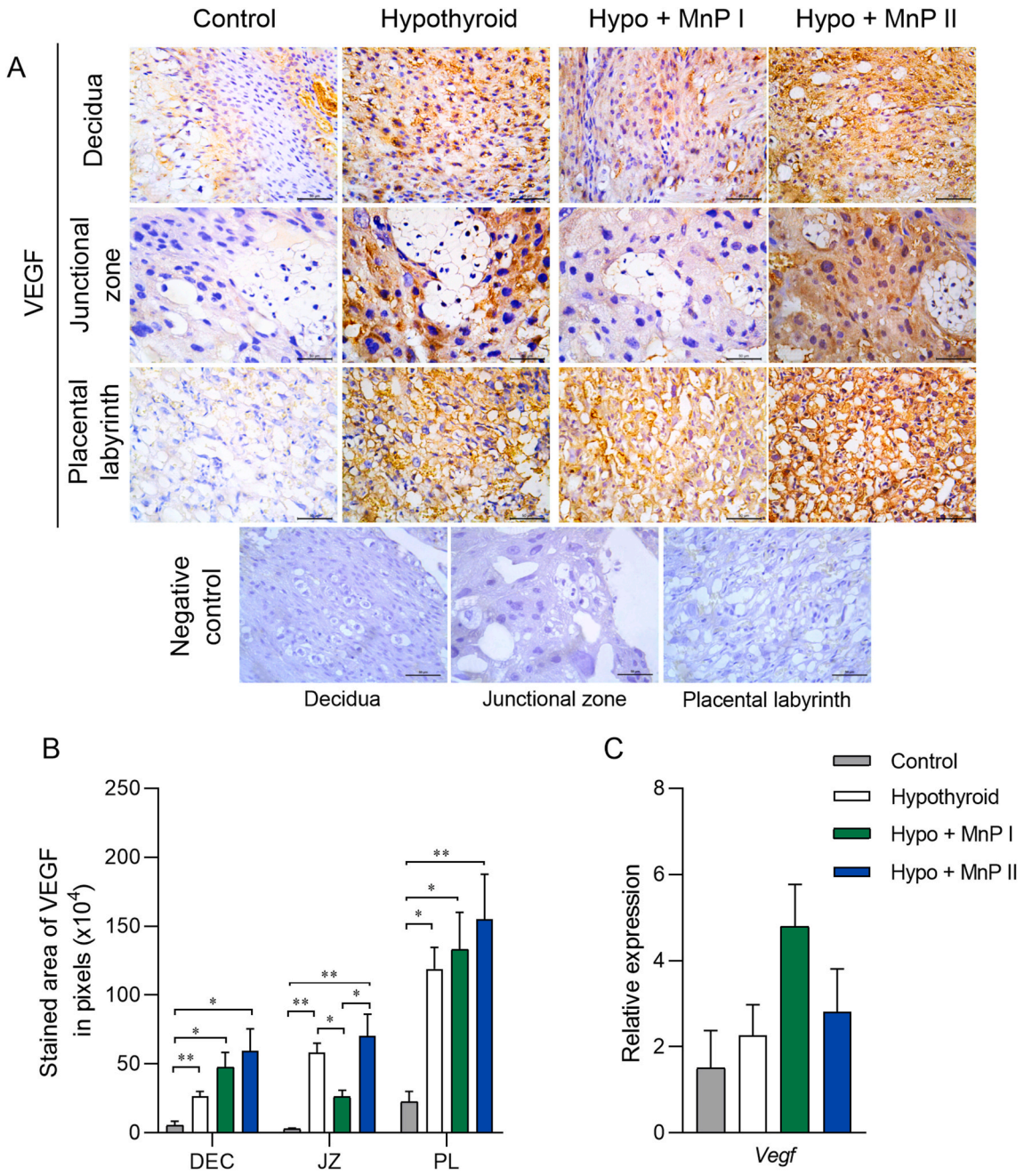

Fig. 7. Expression of VEGF at the maternal-fetal interface of control, hypothyroid, and hypothyroid rats treated with [MnTE-2-PyP]$^{5+}$ (MnP I) and [MnT (5-Br-3-E-Py)P]$^{5+}$ (MnP II). A) Photomicrographs of the immunostaining of VEGF in the decidua, junctional zone, placental labyrinth, and negative control (streptavidin-biotin-peroxidase, contrasted with Harris hematoxylin, Bar = 50 μm). B) Immunostaining area in pixels of VEGF in the decidua, junctional zone, and placental labyrinth. C) E) Relative gene expression of *Vegf* in the placenta (mean ± SEM, *P < 0.05; **P < 0.01; N = 6–8/group).

maternal-fetal interface, or the plasma levels of hepatic (ALT, AST, alkaline phosphatase, total proteins, albumin) and renal (urea, creatinine) biomarkers. Furthermore, MnP I reduced the levels of creatine kinase, a biomarker of muscle injury when values are high [79], while MnP II did not change this parameter. Together, these data suggest that the use of MnPs at a dose of 0.1 mg/kg/day and from the 8th day of gestation is safe for fetal and placental development in the animal model used.

By administering MnPs I and II in rats with maternal hypothyroidism, we demonstrated that the use of both not only increased the fetal body mass and improved the relative frequency of fetal body mass distribution of hypothyroid rats, but MnP I also increased the mass of fetal organs, showing better effects on fetal development compared to MnP II according to PCA analysis. The increase in fetal body mass and the fetal organs such as liver, kidneys, heart, and lungs is important for the proper development of the fetus, as intrauterine development and size at birth are determining factors of postnatal health [80].

The improved fetal development of hypothyroid rats caused by MnPs was also associated with improved placental morphology and vascularization since the MnPs restored the population of glycogen cells in the JZ of hypothyroid rats and increased the area occupied by maternal vascular sinus and fetal capillary in the PL. The increase in glycogen cells in the placenta of hypothyroid rats of the present study has also been described by Ref. [47]. The normalization of this cell population caused by treatment with MnPs suggests the reestablishment of adequate differentiation of trophoblast cells during the formation and development

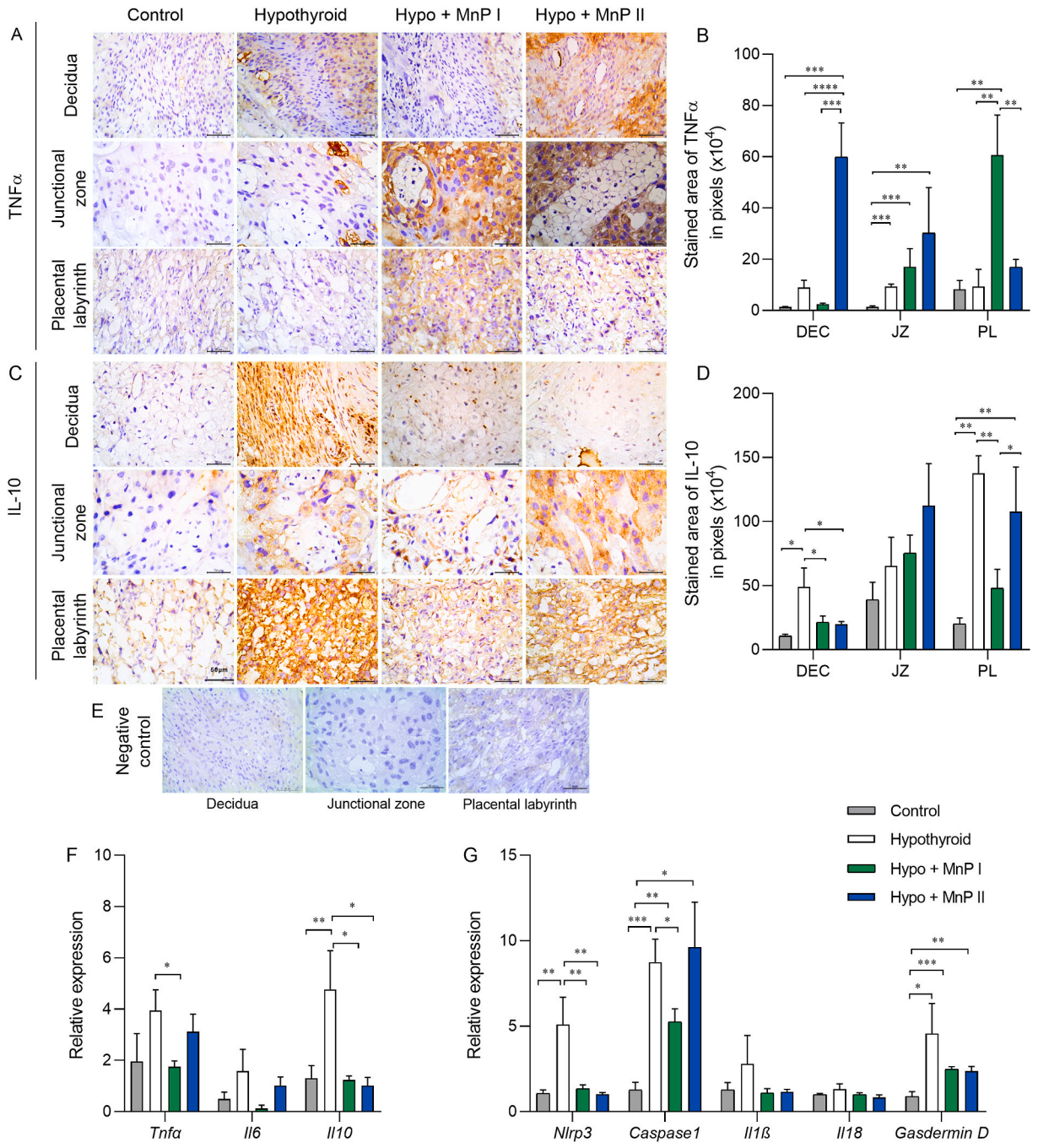

Fig. 8. Expression of TNFα, IL10, IL6, and mediators of the inflammasome-NLRP3 via and pyroptosis at the maternal-fetal interface of control, hypothyroid, and hypothyroid rats treated with $[MnTE\text{-}2\text{-}PyP]^{5+}$ (MnP I) and $[MnT(5\text{-}Br\text{-}3\text{-}E\text{-}Py)P]^{5+}$ (MnP II). A, C) Photomicrographs of the immunostaining of TNFα (A), and IL10 (C) in the decidua, junctional zone, and placental labyrinth (streptavidin-biotin-peroxidase, contrasted with Harris hematoxylin, Bar = 50 μm). B, D) Immunostaining area in pixels of TNFα (B), and IL10 (D) in the decidua, junctional zone, and placental labyrinth. E) Negative Control. F) Relative gene expression of *Tnf, Il6, and Il10* in the placenta. G) Relative gene expression of *Nlrp3, Caspase1, Il1β, Il18, and Gasdermin D* in the placenta (mean ± SEM, *P < 0.05; **P < 0.01; ***P < 0.001; ****P < 0.0001; SNK test; N = 6–8/group).

of the placenta and/or its adequate migration towards the decidua. In addition, studies have suggested that alterations in glycogen cell populations are in the genesis of gestational diseases in experimental models, especially when there is altered fetal growth [81]. Therefore, the improvement in this cell population after treatment with MnPs may have contributed to the increase in fetal body mass observed. The greater vascularization in the placenta of hypothyroid rats caused by MnPs also favors higher fetal body mass since it allows a greater supply of oxygen and nutrients to the developing fetus. Corroborating our results [82], demonstrate *in vitro* an increase in angiogenesis in human umbilical cord endothelial cells (HUVECs) when treated with another MnP formulation (MnTBAP), suggesting a pro-angiogenic effect of this MnP. However, some studies have also demonstrated the anti-angiogenic action of some MnPs (e.g. $[MnTE\text{-}2\text{-}PyP]^{5+}$, $[MnTnHex\text{-}2\text{-}PyP]^{5+}$) in cancer and radiotherapy models [39,66,83].

In addition to the improved placental morphology and vascularization, MnPs were able to reduce placental and/or decidual expression of HIF1α, a biomarker of cellular hypoxia [64,84], and 8-OHdG and MDA, markers of oxidative DNA damage and lipid peroxidation, respectively [67,68]. In a previous study, MnP I reduced the protein expression of

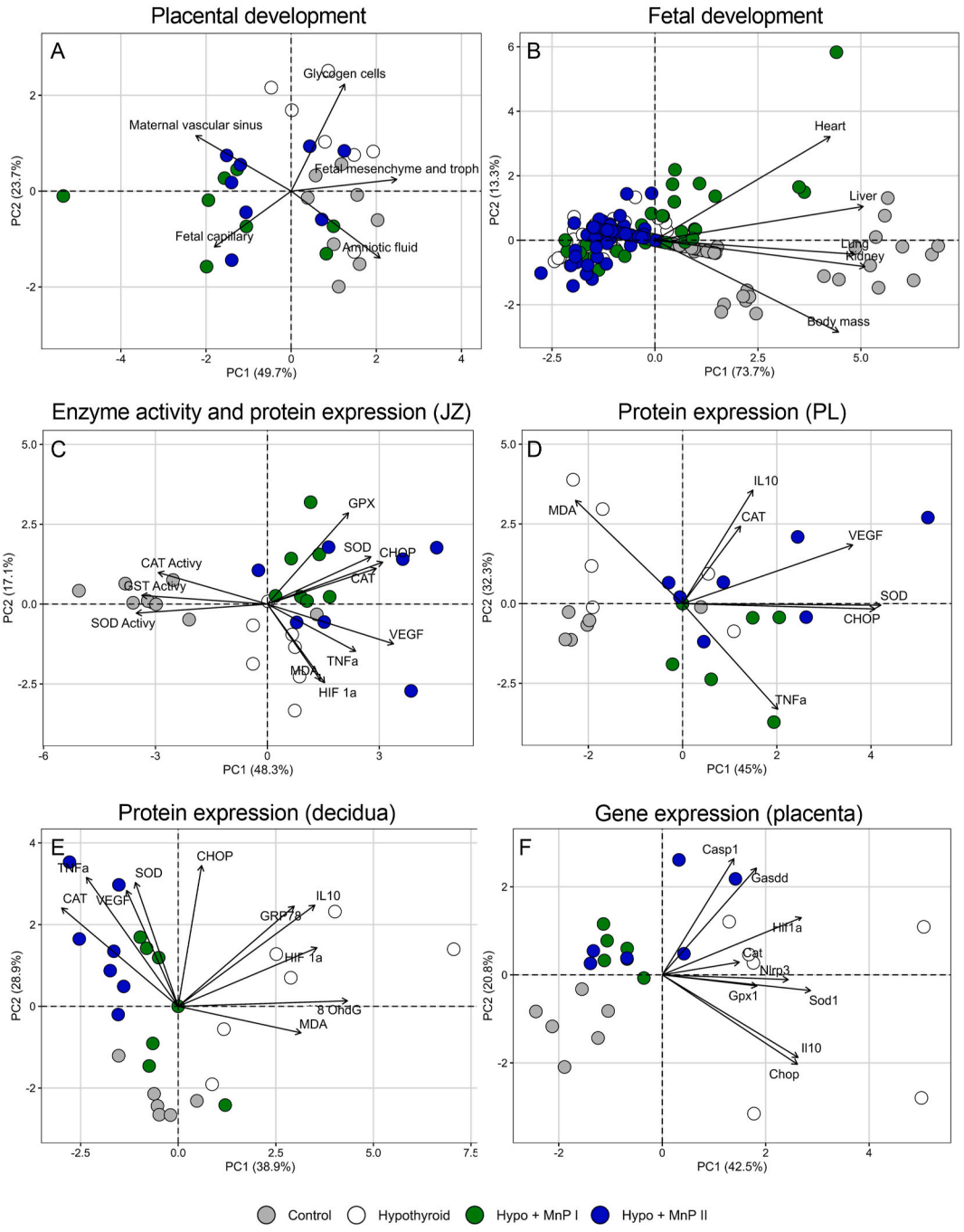

Fig. 9. PCA analysis on placental and fetal development, antioxidant activity and gene and protein expression at the maternal-fetal interface of control, hypothyroid, and hypothyroid rats treated with [MnTE-2-PyP]$^{5+}$ (MnP I) and [MnT(5-Br-3-E-Py)P]$^{5+}$ (MnP II). A) Placental development; B) Fetal development; C) Antioxidant enzyme activity and protein expression in the junctional zone (JZ); D) Protein expression in the placental labyrinth (PL); E) Protein expression in the decidua; F) Gene expression in the placenta.

8-OHdG, and HIF1α in 4T1 orthotopic mammary carcinomas in Balb/c mice, suggesting reduced hypoxia and oxidative stress in this experimental model [85]. Moreover [39], demonstrated a reduction in the immunostaining of HIF1α and 8-OHdG in a radiation-induced lung injury model in rats using the same metalloporphyrin. Taken together, our results suggest that MnPs I and II have protective effects against hypoxia and placental oxidative stress caused by maternal hypothyroidism, as was also demonstrated in the PCA analysis. Moreover, they show that MnP II, which until now had not been evaluated *in vitro* and *in vivo*, has cytoprotective effects similar to MnP I against oxidative stress.

The reduced hypoxia and oxidative damage in the maternal-fetal interface of hypothyroid rats in the present study may be the result of increased placental vascularization caused by MnPs I and II, allowing greater oxygen supply to the maternal-fetal interface. Furthermore, this reduction may be caused by the direct action of these MnPs, which are SOD mimics and have potent catalytic action of reactive oxygen and nitrogen species, especially superoxide and peroxynitrite [85]. Treatment with MnPs I and II has not been able to increase the placental gene expression of *Nrf2* in rats with hypothyroidism, a transcription factor involved in the expression of antioxidant enzymes [86], or alter placental levels of ROS and peroxynitrite. However, in the hypothyroid rats, although treatment with MnPs I and II did not increase the

placental enzyme activity of SOD, catalase, and GST, both metalloporphyrins were able to increase placental and/or decidual protein expression of SOD1 and GPx1/2, which are important antioxidant enzymes involved in the control of ROS in biological systems [87,88]. Interestingly, MnP II, unlike MnP I, was also able to increase decidual and placental catalase protein expression, demonstrating that in the maternal-fetal interface of rats, MnP II has a greater potential to increase antioxidant enzymes than MnP I. In addition, both metalloporphyrins were able to restore placental gene expression of *Gpx1*, matching the control, and reduce the higher gene expression of *Sod1* caused by hypothyroidism, demonstrating the potential of these MnPs in regulating the cellular redox state.

Our results regarding the immunostaining and gene expression of antioxidant enzymes are consistent with those of [89]. According to these authors, pretreatment with $[MnTM\text{-}4\text{-}PyP]^{5+}$ in an *in vitro* model of oxidative stress using rat cortical neurons exposed to hydrogen peroxide (H_2O_2) significantly increased protein levels of SOD1, SOD2, and CAT and reduced the gene expression of *Sod1* and *Cat*. A previous study conducted by Ref. [90] also showed that *in vitro* and *in vivo* treatment with another MnP ($[MnT\textit{n}BuOE\text{-}2\text{-}PyP]^{5+}$) increased gene and/or protein expression of Cat and SOD in bone marrow cells of C57BL/6 mice. Thus, our results suggest that treatment with MnPs I and II protects against oxidative stress at the maternal-fetal interface of hypothyroid rats. In this regard, treatment not only reduced the expression of HIF1α, 8-OHdG, and MDA, but also increased the placental and/or decidual protein expression of SOD1, catalase, and GPx1/2 and restored the placental gene expression of *Sod1* and *Gpx1*.

In addition to evaluating the potential of MnPs I and II to protect against oxidative stress at the maternal-fetal interface caused by hypothyroidism [11], we analyzed its protective effects against endoplasmic reticulum stress, another biological process involved in cell damage that can be caused by oxidative stress [91]. To date, endoplasmic reticulum stress has not been studied in *in vivo* models to evaluate the MnPs, while a previous study demonstrated the occurrence of this process in the placenta and decidua of hypothyroid rats [11]. MnPs I and/or II reduced the higher decidual protein expression of GRP78 and CHOP caused by hypothyroidism in rats, as well as the placental gene expression of *Chop*, matching the control. Our results are consistent with those of *in vitro* studies of oxidative stress, in which reduced expression of GRP78 and/or CHOP was observed after treatment with a $[MnTM\text{-}4\text{-}PyP]^{5+}$ in rat primary cortical neurons exposed to H_2O_2 [89] and after the administration of $[MnTM\text{-}4\text{-}PyP]^{5+}$ in lung adenocarcinoma cells (A549) exposed to paraquat [91]. GRP78 and CHOP are markers of endoplasmic reticulum stress activation [73,74]. Some studies have described the increased expression of these mediators in severe gestational diseases such as miscarriage, preeclampsia, and IUGR [1,2,92,93]. These findings suggest the protective effect of MnPs I and II against endoplasmic reticulum stress at the maternal-fetal interface of hypothyroid rats.

The activation of oxidative stress and endoplasmic reticulum stress can alter the expression of angiogenic and immunological mediators [64,92,94,95], which are critical for proper placental function [48,96,97]. Interestingly, treatment with MnP I reduced the higher VEGF immunostaining in the JZ of hypothyroid rats, while both metalloporphyrins were not able to reduce the higher VEGF expression caused by hypothyroidism in the decidua and PL. VEGF is one of the main pro-angiogenic mediators in the maternal-fetal interface, especially in the first and second trimesters of pregnancy [98]. However, VEGF expression is also an indicator of hypoxia since it is activated via HIF1α in a low oxygen environment [75]. Therefore, the reduced VEGF expression in the JZ caused by MnP I may reflect the inhibition of HIF1α expression caused by this metalloporphyrin in hypothyroid rats. Our results are in accordance with [85], who also demonstrated reduced VEGF expression in a murine model of breast tumor after treatment with MnP I associated with reduced HIF1α and cellular hypoxia. However, other studies have demonstrated increased VEGF expression in the muscle tissue of mice treated with MnTBAP and subjected to revascularization under ischemic conditions [82], as was also noted by Ref. [39] in a model of radiation-induced lung injury after treatment with MnP I. Thus, further studies are needed to clarify the role of MnPs in modulating VEGF expression in biological systems.

Regarding immunological mediators, the administration of MnPs I and II increased the expression of TNFα in the PL and decidua, respectively, as was also observed in the PCA analysis, while in the JZ, the MnPs did not alter the higher expression of TNFα caused by hypothyroidism. However, MnP I reduced placental gene expression of *Tnf*. An *in vitro* study also showed reduced TNFα expression in murine macrophages (RAW 264.7) exposed to lipopolysaccharide (LPS) and treated with MnTBAP [99]. This result was also observed *in vivo* in a renal ischemia/reperfusion model in rats treated with a $[MnTM\text{-}4\text{-}PyP]^{5+}$ [100]. On the other hand, both metalloporphyrins reduced the higher decidual expression of IL-10 caused by hypothyroidism, matching the control, as also occurred in the PL with the administration of MnP I. Thus, the reduction of IL-10 caused by MnPs may have contributed to the increase in TNFα since IL-10 essentially suppresses pro-inflammatory cytokines [96,97,101]. Furthermore, the reduced IL-10 expression at the control level caused by MnPs suggests a positive modulation of these metalloporphyrins on the placental immune profile of hypothyroid rats.

In addition, both metalloporphyrins were not able to reduce the higher placental gene expression of *Nlrp3* caused by hypothyroidism, matching the control, while MnP I also reduced the higher *Caspase1* gene expression, mediators involved in the NLRP3 inflammasome activation. However, the use of these MnPs did not reduce the increased gene expression of *Gasdermin d*, a mediator of pyroptosis, caused by hypothyroidism [78]. demonstrated recently that maternal hypothyroidism activates the NLRP3 inflammasome and pyroptosis in the placenta and decidua of rats, and this pathway is also involved in the placental dysfunctions seen in miscarriage, preeclampsia, and gestational diabetes [102–106]. A previous study conducted by Ref. [107] also showed that *in vivo* treatment with $[MnTE\text{-}2\text{-}PyP]^{5+}$ (MnP I) attenuated NLRP3 inflammasome activation in pulmonary hypertension murine model, corroborating the results of the present study.

Among the main limitations of this study was the impossibility of analyzing redox and UPR mediators according to the sex of the maternal-fetal unit, which can influence the results, since studies have shown sex-specific differences in the expression of these placental mediators in models of gestational hypoxia and alimentary intrauterine growth restriction [108,109]. Furthermore, assessments during the formation of the definitive placenta and the beginning of the fetal exponential growth (12–14 DG) [110] would allow a better understanding of the effects of MnPs on the placental redox environment.

This study demonstrated that $[MnTE\text{-}2\text{-}PyP]^{5+}$ and $[MnT(5\text{-}Br\text{-}3\text{-}E\text{-}Py)P]^{5+}$ improves the fetal-placental development of hypothyroid rats and protects against oxidative stress and endoplasmic reticulum stress caused by hypothyroidism at the maternal-fetal interface, with $[MnTE\text{-}2\text{-}PyP]^{5+}$ showing better effects than $[MnT(5\text{-}Br\text{-}3\text{-}E\text{-}Py)P]^{5+}$. The findings also showed that this treatment restores the placental and/or decidual expression of IL10 and reduces *Nlrp3* and *Caspase1*, suggesting potential therapeutic alternatives for gestational dysfunctions that occur with placental stress and NLRP3 inflammasome activation.

Funding

This work was supported by *Conselho Nacional de Desenvolvimento Científico e Tecnológico* (CNPq), *Universidade Estadual de Santa Cruz* (UESC), *Coordenação de Aperfeiçoamento de Pessoal de Nível Superior* (Capes), *Fundação de Amparo à Pesquisa do Estado de Minas Gerais* (FAPEMIG).

CRediT authorship contribution statement

Jeane Martinha dos Anjos Cordeiro: Writing – original draft,

Methodology, Investigation, Formal analysis, Data curation. **Luciano Cardoso Santos:** Methodology, Investigation, Data curation. **Bianca Reis Santos:** Methodology, Investigation, Formal analysis, Data curation. **Acácia Eduarda de Jesus Nascimento:** Methodology, Investigation, Data curation. **Emilly Oliveira Santos:** Methodology, Investigation, Data curation. **Erikles Macêdo Barbosa:** Methodology, Investigation, Data curation. **Isabela Oliveira de Macêdo:** Methodology, Investigation, Data curation. **Letícia Dias Mendonça:** Methodology, Investigation, Data curation. **José Ferreira Sarmento-Neto:** Writing – review & editing, Resources, Formal analysis. **Clarice Santos Pinho:** Methodology, Investigation. **Erick Teixeira dos Santos Coura:** Methodology, Investigation. **Acácio de Sá Santos:** Formal analysis, Methodology. **Marciel Elio Rodrigues:** Formal analysis, Methodology. **Júlio Santos Rebouças:** Writing – review & editing, Resources, Methodology, Investigation. **Gilson De-Freitas-Silva:** Writing – review & editing, Resources, Methodology, Funding acquisition. **Alexandre Dias Munhoz:** Resources, Methodology. **Mário Sérgio Lima de Lavor:** Writing – review & editing, Resources, Funding acquisition. **Juneo Freitas Silva:** Writing – review & editing, Writing – original draft, Validation, Supervision, Resources, Project administration, Methodology, Investigation, Funding acquisition, Formal analysis, Data curation, Conceptualization.

Declaration of competing interest

The authors declare that they have no known competing financial interests or personal relationships that could have appeared to influence the work reported in this paper.

Data availability

Data will be made available on request.

Acknowledgements

The authors thank National Institute of Science and Technology in Molecular Sciences (INCT-CiMOL), and Ivo Arouca (Universidade Estadual de Santa Cruz) by the technical support provided. We also thank the LAREMAR facilities at UFMG.

Appendix A. Supplementary data

Supplementary data to this article can be found online at https://doi.org/10.1016/j.redox.2024.103238.

References

[1] H.W. Yung, S. Calabrese, D. Hynx, B.A. Hemmings, I. Cetin, D.S. Charnock-Jones, G.J. Burton, Evidence of placental Translation inhibition and endoplasmic reticulum stress in the etiology of human intrauterine growth restriction, Am. J. Pathol. 173 (2008) 451–462, https://doi.org/10.2353/AJPATH.2008.071193.

[2] G.J. Burton, H.W. Yung, Endoplasmic reticulum stress in the pathogenesis of early-onset pre-eclampsia, Pregnancy Hypertens 1 (2011) 72–78, https://doi.org/10.1016/j.preghy.2010.12.002.

[3] G.J. Burton, H.W. Yung, T. Cindrova-Davies, D.S. Charnock-Jones, Placental endoplasmic reticulum stress and oxidative stress in the pathophysiology of unexplained intrauterine growth restriction and early onset preeclampsia, Placenta 30 (2009) 43, https://doi.org/10.1016/J.PLACENTA.2008.11.003.

[4] G.J. Burton, T. Cindrova-Davies, H. wa Yung, E. Jauniaux, Hypoxia and reproductive health: oxygen and development of the human placenta, Reproduction 161 (2021) F53–F65, https://doi.org/10.1530/REP-20-0153.

[5] F. Folli, D. Corradi, P. Fanti, A. Davalli, A. Paez, A. Giaccari, C. Perego, G. Muscogiuri, The role of oxidative stress in the pathogenesis of type 2 diabetes mellitus micro- and macrovascular complications: avenues for a mechanistic-based therapeutic approach, Curr. Diabetes Rev. 7 (2012) 313–324, https://doi.org/10.2174/157339911797415585.

[6] F. Giacco, M. Brownlee, Oxidative stress and diabetic complications, Circ. Res. 107 (2010) 1058–1070, https://doi.org/10.1161/CIRCRESAHA.110.223545.

[7] I.A. Lian, M. Løset, S.B. Mundal, M.H. Fenstad, M.P. Johnson, I.P. Eide, L. Bjørge, K.A. Freed, E.K. Moses, R. Austgulen, Increased endoplasmic reticulum stress in decidual tissue from pregnancies complicated by fetal growth restriction with and without pre-eclampsia, Placenta 32 (2011) 823–829, https://doi.org/10.1016/j.placenta.2011.08.005.

[8] I. Idris, R. Srinivasan, A. Simm, R.C. Page, Maternal hypothyroidism in early and late gestation: effects on neonatal and obstetric outcome, Clin, Endocrinol. (Oxf). 63 (2005) 560–565, https://doi.org/10.1111/j.1365-2265.2005.02382.x.

[9] H. Zhang, Y. Dong, Q. Su, Perinatal Hypothyroidism Modulates Antioxidant Defence Status in the Developing Rat Liver and Heart, vol. 95, 2016, pp. 185–189, https://doi.org/10.1139/CJPP-2016-0177, 10.1139/Cjpp-2016-0177.

[10] R.K. Sahay, V.S. Nagesh, Hypothyroidism in pregnancy, Indian J. Endocrinol. Metab. 16 (n.d.). https://doi.org/10.4103/2230-8210.95667.

[11] J.M. dos Anjos Cordeiro, L.C. Santos, L.S. de Oliveira, B.R. Santos, E.O. Santos, E. M. Barbosa, I.O. de Macêdo, G.J.C. de Freitas, D. de A. Santos, M.S.L. de Lavor, J. F. Silva, Maternal hypothyroidism causes oxidative stress and endoplasmic reticulum stress in the maternal-fetal interface of rats, Free Radic. Biol. Med. 191 (2022) 24–39, https://doi.org/10.1016/j.freeradbiomed.2022.08.033.

[12] C. Longcope, The male and female reproductive systems, in: Berne & Amp Levy Physiol., JB Lippincott Co, 2010, pp. 758–798, https://doi.org/10.1016/b978-0-323-07362-2.50047-4.

[13] S. Thangaratinam, A. Tan, E. Knox, M.D. Kilby, J. Franklyn, A. Coomarasamy, Association between thyroid autoantibodies and miscarriage and preterm birth: meta-analysis of evidence, BMJ 342 (2011), https://doi.org/10.1136/BMJ.D2616.

[14] B. Larijani, V. Marsoosi, S. Aghakhani, A. Moradi, S. Hashemipour, Thyroid Hormone Alteration in Pre-eclamptic Women, vol. 18, 2009, pp. 97–100, https://doi.org/10.1080/09513590310001652973, 10.1080/0951359031000165297 3.

[15] L.O. Kurlak, H.D. Mistry, E. Kaptein, T.J. Visser, F. Broughton Pipkin, Thyroid hormones and their placental deiodination in normal and pre-eclamptic pregnancy, Placenta 34 (2013) 395–400, https://doi.org/10.1016/J.PLACENTA.2013.02.009.

[16] G.E. Krassas, Thyroid disease and female reproduction, Fertil. Steril. 74 (2000) 1063–1070.

[17] J.F. Silva, N.M. Ocarino, R. Serakides, Thyroid hormones and female reproduction, Biol. Reprod. 99 (2018) 907–921, https://doi.org/10.1093/biolre/ioy115.

[18] J.F. Silva, P.N. Vidigal, D.D. Galvo, J.N. Boeloni, P.P. Nunes, N.M. Ocarino, E. F. Nascimento, R. Serakides, Fetal growth restriction in hypothyroidism is associated with changes in proliferative activity, apoptosis and vascularisation of the placenta, Reprod. Fertil. Dev. 24 (2012) 923–931, https://doi.org/10.1071/RD11219.

[19] J.F. Silva, N.M. Ocarino, R. Serakides, Maternal thyroid dysfunction affects placental profile of inflammatory mediators and the intrauterine trophoblast migration kinetics, Reproduction 147 (2014) 803–816, https://doi.org/10.1530/REP-13-0374.

[20] J.F. Silva, N.M. Ocarino, R. Serakides, Placental angiogenic and hormonal factors are affected by thyroid hormones in rats, Pathol. Res. Pract. 211 (2015) 226–234, https://doi.org/10.1016/J.PRP.2014.11.003.

[21] D.K. Sahoo, A. Roy, S. Bhanja, G.B.N. Chainy, Hypothyroidism impairs antioxidant defence system and testicular physiology during development and maturation, Gen. Comp. Endocrinol. 156 (2008) 63–70, https://doi.org/10.1016/J.YGCEN.2007.11.007.

[22] L. Meng, E. Rijntjes, H. Swarts, A. Bunschoten, I. van der Stelt, J. Keijer, K. Teerds, Dietary-induced chronic hypothyroidism negatively affects rat follicular development and ovulation rate and is associated with oxidative stress, Biol. Reprod. 94 (2016), https://doi.org/10.1095/biolreprod.115.136515.

[23] S.K. Chakrabarti, S. Ghosh, S. Banerjee, S. Mukherjee, S. Chowdhury, Oxidative stress in hypothyroid patients and the role of antioxidant supplementation, Indian J. Endocrinol. Metab 20 (2016) 674, https://doi.org/10.4103/2230-8210.190555.

[24] A. Mancini, C. Di Segni, S. Raimondo, G. Olivieri, A. Silvestrini, E. Meucci, D. Currò, Thyroid hormones, oxidative stress, and inflammation, Mediators Inflamm (2016) 2016, https://doi.org/10.1155/2016/6757154.

[25] S.R. Hansson, Å. Nääv, L. Erlandsson, Oxidative stress in preeclampsia and the role of free fetal hemoglobin, Front. Physiol. 6 (2015) 516, https://doi.org/10.3389/FPHYS.2014.00516/BIBTEX.

[26] R. Aouache, L. Biquard, D. Vaiman, F. Miralles, Oxidative stress in preeclampsia and placental diseases, Int. J. Mol. Sci. 19 (2018) 1496, https://doi.org/10.3390/IJMS19051496, 2018, Vol. 19, Page 1496.

[27] I. Batinic-Haberle, I. Spasojevic, H.M. Tse, A. Tovmasyan, Z. Rajic, D.K.S. Clair, Z. Vujaskovic, M.W. Dewhirst, J.D. Piganelli, Design of Mn porphyrins for treating oxidative stress injuries and their redox-based regulation of cellular transcriptional activities, Amino Acids 42 (2012) 95, https://doi.org/10.1007/S00726-010-0603-6.

[28] A. Chatterjee, E.A. Kosmacek, S. Shrishrimal, J.T. McDonald, R.E. Oberley-Deegan, MnTE-2-PyP, a manganese porphyrin, reduces cytotoxicity caused by irradiation in a diabetic environment through the induction of endogenous antioxidant defenses, Redox Biol. 34 (2020) 101542, https://doi.org/10.1016/J.REDOX.2020.101542.

[29] I. Batinic-Haberle, A. Tovmasyan, E.R.H. Roberts, Z. Vujaskovic, K.W. Leong, I. Spasojevic, SOD therapeutics: latest insights into their structure-activity relationships and impact on the cellular redox-based signaling pathways, Antioxid. Redox Signal. 20 (2014) 2372, https://doi.org/10.1089/ARS.2012.5147.

[30] I. Batinic-Haberle, Z. Rajic, L. Benov, A combination of two antioxidants (an SOD mimic and ascorbate) produces a pro-oxidative effect forcing Escherichia coli to

adapt via induction of oxyR regulon, Anti Cancer Agents Med. Chem. 11 (2012) 329–340, https://doi.org/10.2174/187152011795677562.
[31] I. Batinić-Haberle, S. Cuzzocrea, J.S. Rebouças, G. Ferrer-Sueta, E. Mazzon, R. Di Paola, R. Radi, I. Spasojević, L. Benov, D. Salvemini, I. Batinic-Haberle, Pure MnTBAP selectively scavenges peroxynitrite over superoxide: comparison of pure and commercial MnTBAP samples to MnTE-2-PyP in two different models of oxidative stress injuries, SOD-specific E. coli model and carrageenan-induced pleurisy, Free Radic. Biol. Med. 46 (2009) 192–201, https://doi.org/10.1016/j.freeradbiomed.2008.09.042.
[32] K.R. Olson, Y. Gao, A.K. Steiger, M.D. Pluth, C.R. Tessier, T.A. Markel, D. Boone, R.V. Stahelin, I. Batinic-Haberle, K.D. Straubg, Effects of manganese porphyrins on cellular sulfur metabolism, Mol 25 (2020) 980, https://doi.org/10.3390/MOLECULES25040980, 2020, Vol. 25, Page 980.
[33] S. Shrishrimal, A. Chatterjee, E.A. Kosmacek, P.J. Davis, J.T. McDonald, R. E. Oberley-Deegan, Manganese porphyrin, MnTE-2-PyP, treatment protects the prostate from radiation-induced fibrosis (RIF) by activating the NRF2 signaling pathway and enhancing SOD2 and sirtuin activity, Free Radic. Biol. Med. 152 (2020) 255, https://doi.org/10.1016/J.FREERADBIOMED.2020.03.014.
[34] I. Batinic-Haberle, A. Tovmasyan, Z. Huang, W. Duan, L. Du, S. Siamakpour-Reihani, Z. Cao, H. Sheng, I. Spasojevic, A. Alvarez Secord, H2O2-Driven anticancer activity of Mn porphyrins and the underlying molecular pathways, Oxid. Med. Cell. Longev. 2021 (2021), https://doi.org/10.1155/2021/6653790.
[35] S.C. Gad, D.W. Sullivan, I. Spasojevic, C.V. Mujer, C.B. Spainhour, J.D. Crapo, Nonclinical safety and toxicokinetics of MnTnBuOE-2-PyP5+ (BMX-001), Int. J. Toxicol. 35 (2016) 438–453, https://doi.org/10.1177/1091581816642766.
[36] S.C. Gad, D.W. Sullivan, J.D. Crapo, C.B. Spainhour, A nonclinical safety assessment of MnTE-2-PyP, a manganese porphyrin, Int. J. Toxicol. 32 (2013) 274–287, https://doi.org/10.1177/1091581813490203.
[37] S.C. Gad, D.W. Sullivan, C.V. Mujer, C.B. Spainhour, J.D. Crapo, Nonclinical safety and toxicokinetics of MnTE-2-PyP (BMX-010), a topical agent in phase 2 trials for psoriasis and atopic dermatitis, Int. J. Toxicol. 38 (2019) 291–302, https://doi.org/10.1177/1091581819852325.
[38] R. Bottino, A.N. Balamurugan, H. Tse, C. Thirunavukkarasu, X. Ge, J. Profozich, M. Milton, A. Ziegenfuss, M. Trucco, J.D. Piganelli, Response of human islets to isolation stress and the effect of antioxidant treatment, Diabetes 53 (2004) 2559–2568, https://doi.org/10.2337/DIABETES.53.10.2559.
[39] B. Gauter-Fleckenstein, K. Fleckenstein, K. Owzar, C. Jiang, J.S. Rebouças, I. Batinic-Haberle, Z. Vujaskovic, Early and late administration of MnTE-2-PyP5+ in mitigation and treatment of radiation-induced lung damage, Free Radic. Biol. Med. 48 (2010) 1034–1043, https://doi.org/10.1016/J.FREERADBIOMED.2010.01.020.
[40] P. Jungsuwadee, M.R. Weaver, F. Gally, R.E. Oberley-Deegan, The metalloporphyrin antioxidant, MnTE-2-PyP, inhibits Th2 cell immune responses in an asthma model, Int. J. Mol. Sci. 13 (2012) 9785–9797, https://doi.org/10.3390/IJMS13089785, 2012, Vol. 13, Pages 9785-9797.
[41] I. Batinić-Haberle, I. Spasojević, P. Hambright, L. Benov, A.L. Cmmbliss, I. Fridovich, Relationship among redox potentials, proton dissociation constants of pyrrolic nitrogens, and in vivo and in vitro superoxide dismutating activities of manganese(III) and iron(III) water-soluble porphyrins, Inorg. Chem. 38 (1999) 4011–4022, https://doi.org/10.1021/ic990118k.
[42] J.S. Rebouças, I. Kos, Z. Vujasković, I. Batinić-Haberle, Determination of residual manganese in Mn porphyrin-based superoxide dismutase (SOD) and peroxynitrite reductase mimics, J. Pharm. Biomed. Anal. 50 (2009) 1088, https://doi.org/10.1016/J.JPBA.2009.07.002.
[43] J.S. Rebouças, I. Spasojević, I. Batinić-Haberle, Quality of potent Mn porphyrin-based SOD mimics and peroxynitrite scavengers for pre-clinical mechanistic/therapeutic purposes, J. Pharm. Biomed. Anal. 48 (2008) 1046, https://doi.org/10.1016/J.JPBA.2008.08.005.
[44] V.H.A. Pinto, D. CarvalhoDa-Silva, J.L.M.S. Santos, T. Weitner, M.G. Fonseca, M. I. Yoshida, Y.M. Idemori, I. Batinić-Haberle, J.S. Rebouças, Thermal stability of the prototypical Mn porphyrin-based superoxide dismutase mimic and potent oxidative-stress redox modulator Mn(III) meso-tetrakis(N-ethylpyridinium-2-yl) porphyrin chloride, MnTE-2-PyP5+, J. Pharm. Biomed. Anal. 73 (2013) 29, https://doi.org/10.1016/J.JPBA.2012.03.033.
[45] P. Hambright, A. Adeyemo, A. Shamim, S. Lemelle, D.K. Lavallee, D. Miller, A. White, [[4,4′4″,4‴-Porphyrin-5,10,15, 20-tetrayltetrakis(1-methylpyridiniumato](2-)]- indium(III) pentaperchlorate, Inorg. Synth. 23 (1985) 55–59, https://doi.org/10.1002/9780470132548.CH14.
[46] J.F. Silva, R. Serakides, Intrauterine trophoblast migration: a comparative view of humans and rodents, Cell Adh, Migr. 10 (2016) 88, https://doi.org/10.1080/19336918.2015.1120397.
[47] J.F. Silva, P.N. Vidigal, D.D. Galvão, J.N. Boeloni, P.P. Nunes, N.M. Ocarino, E. F. Nascimento, R. Serakides, Fetal growth restriction in hypothyroidism is associated with changes in proliferative activity, apoptosis and vascularisation of the placenta, Reprod. Fertil. Dev. 24 (2012) 923, https://doi.org/10.1071/RD11219.
[48] B.R. Santos, J.M. dos A. Cordeiro, L.C. Santos, E.O. Santos, L.S. de Oliveira, E. M. Barbosa, I.O. Macedo, J.F. Sarmento-Neto, J.S. Rebouças, G. de F. Silva, J. F. Silva, Manganese porphyrin-based treatment blocks placental stress caused by maternal hypothyroidism and improves placental morphogenesis and fetal development in a rat experimental model, in: XX Congr. Brazilian Soc. Cell Biol., Brazilian Society for Cell Biology, São Paulo, 2021, pp. 231–232.
[49] M. Ilie, S. Khambata-Ford, C. Copie-Bergman, L. Huang, J. Juco, V. Hofman, P. Hofman, G. Henri, M.-A. Chenevier, Use of the 22C3 anti-PD-L1 antibody to determine PD-L1 expression in multiple automated immunohistochemistry platforms. https://doi.org/10.1371/journal.pone.0183023, 2017.
[50] M.E. Solano, K. Thiele, M.K. Kowal, P.C. Arck, Identification of suitable reference genes in the mouse placenta, Placenta 39 (2016) 7–15, https://doi.org/10.1016/J.PLACENTA.2015.12.017.
[51] M.M. Bradford, A rapid and sensitive method for the quantitation of microgram quantities of protein utilizing the principle of protein-dye binding, Anal. Biochem. 72 (1976) 248–254, https://doi.org/10.1016/0003-2697(76)90527-3.
[52] W.H. Habig, M.J. Pabst, W.B. Jakoby, Glutathione S-transferases, J. Biol. Chem. 249 (1974) 7130–7139.
[53] S. Marklund, G. Marklund, Involvement of the superoxide anion radical in the autoxidation of pyrogallol and a convenient assay for superoxide dismutase, Eur. J. Biochem. 47 (1974) 469–474, https://doi.org/10.1111/j.1432-1033.1974.tb03714.x.
[54] H. Aebi, Catalase in vitro, Methods Enzymol. 105 (1984) 121–126, https://doi.org/10.1016/S0076-6879(84)05016-3.
[55] G.F. Ferreira, L. de M. Baltazar, J.R. Alves Santos, A.S. Monteiro, L.A. de O. Fraga, M.A. Resende-Stoianoff, D.A. Santos, The role of oxidative and nitrosative bursts caused by azoles and amphotericin B against the fungal pathogen Cryptococcus gattii, J. Antimicrob. Chemother. 68 (2013) 1801–1811, https://doi.org/10.1093/JAC/DKT114.
[56] D.S. Charnock-Jones, Placental hypoxia, endoplasmic reticulum stress and maternal endothelial sensitisation by sFLT1 in pre-eclampsia, J. Reprod. Immunol. 114 (2016) 81–85, https://doi.org/10.1016/J.JRI.2015.07.004.
[57] J. Josse, F. Husson, Handling missing values in exploratory multivariate data analysis methods, J. La Société Française Stat. 153 (2012).
[58] J. Josse, F. Husson, missMDA : a package for handling missing values in multivariate data analysis, J. Stat. Softw. 70 (2016), https://doi.org/10.18637/jss.v070.i01.
[59] F. Husson, Exploratory Multivariate Analysis by Example Using R, CRC Press, 2010, https://doi.org/10.1201/b10345.
[60] M. Gouterman, The Porphyrins. Volume 3, Physical Chemistry. Part A, Academic Press, 1978.
[61] L.J. Boucher, Manganese porphyrin complexes, Coord. Chem. Rev. 7 (1972) 289–329, https://doi.org/10.1016/S0010-8545(00)80024-7.
[62] I. Batinić-Haberle, I. Spasojević, R. Stevens, P. Hambrightc, I. Fridovicha, Supplemental material manganese (III) meso tetrakis ortho N-alkylpyridylporphyrins. Synthesis, characterization, and catalysis of O2.-dismutation, J. Chem. Soc. Dalt. Trans. (2002) 2689–2696.
[63] I. Batinic-Haberle, I. Spasojevic, R.D. Stevens, P. Hambright, P. Neta, A. Okado-Matsumoto, I. Fridovich, Supplemental material new class of potent catalysts O 2 .-Dismutation. Mn(III) ortho-methoxyethylpyridyl- and DI-ortho-methoxyethylimidazolyl porphyrins, J. Chem. Soc. Dalt. Trans. (2004) 30–33.
[64] M.J. Soares, K. Iqbal, K. Kozai, Hypoxia and placental development, Birth Defects Res 109 (2017) 1309–1329, https://doi.org/10.1002/BDR2.1135.
[65] F.V. Francisqueti-Ferron, A.J.T. Ferron, J.L. Garcia, C.C.V. De Almeida Silva, M. R. Costa, C.S. Gregolin, F. Moreto, A.L.A. Ferreira, I.O. Minatel, C.R. Correa, Basic concepts on the role of nuclear factor erythroid-derived 2-like 2 (Nrf2) in age-related diseases, Int. J. Mol. Sci. 20 (2019), https://doi.org/10.3390/IJMS20133208.
[66] B. Gauter-Fleckenstein, J.S. Reboucas, K. Fleckenstein, A. Tovmasyan, K. Owzar, C. Jiang, I. Batinic-Haberle, Z. Vujaskovic, Robust rat pulmonary radioprotection by a lipophilic Mn N-alkylpyridylporphyrin, MnTnHex-2-PyP 5 þ $, (n.d.). https://doi.org/10.1016/j.redox.2013.12.017.
[67] X. Kong, Y. Zhang, H.B. Wu, F.X. Li, D.Y. Zhang, Q. Su, Combination therapy with losartan and pioglitazone additively reduces renal oxidative and nitrative stress induced by chronic high fat, sucrose, and sodium intake, Oxid. Med. Cell. Longev. (2012), https://doi.org/10.1155/2012/856085.
[68] S.K. Urbaniak, K. Boguszewska, M. Szewczuk, J. Kázmierczak-Barańska, B. T. Karwowski, 8-Oxo-7,8-Dihydro-2′-Deoxyguanosine (8-oxodG) and 8-hydroxy-2′-deoxyguanosine (8-OHdG) as a potential biomarker for gestational diabetes mellitus (GDM) development, Mol 25 (2020) 202, https://doi.org/10.3390/MOLECULES25010202, 2020, Vol. 25, Page 202.
[69] H.D. Mistry, P.J. Williams, The importance of antioxidant micronutrients in pregnancy, Oxid. Med. Cell. Longev. (2011), https://doi.org/10.1155/2011/841749.
[70] Y. Sheng, I.A. Abreu, D.E. Cabelli, M.J. Maroney, A.F. Miller, M. Teixeira, J. S. Valentine, Superoxide dismutases and superoxide reductases, Chem. Rev. 114 (2014) 3854–3918, https://doi.org/10.1021/CR4005296.
[71] A. Tovmasyan, C.G.C. Maia, T. Weitner, S. Carballal, R.S. Sampaio, D. Lieb, R. Ghazaryan, I. Ivanovic-Burmazovic, G. Ferrer-Sueta, R. Radi, J.S. Reboucas, I. Spasojevic, L. Benov, I. Batinic-Haberle, A comprehensive evaluation of catalase-like activity of different classes of redox-active therapeutics, Free Radic. Biol. Med. 86 (2015) 308–321, https://doi.org/10.1016/J.FREERADBIOMED.2015.05.018.
[72] D. Rodriguez, D. Rojas-Rivera, C. Hetz, Integrating stress signals at the endoplasmic reticulum: the BCL-2 protein family rheostat, Biochim. Biophys. Acta - Mol. Cell Res. 1813 (2011) 564–574, https://doi.org/10.1016/J.BBAMCR.2010.11.012.
[73] D. Ron, H.P. Harding, Protein-folding homeostasis in the endoplasmic reticulum and nutritional regulation, Cold Spring Harb. Perspect. Biol. 4 (2012), https://doi.org/10.1101/CSHPERSPECT.A013177.
[74] M. Wang, R.J. Kaufman, Protein misfolding in the endoplasmic reticulum as a conduit to human disease, Nat 529 (2016) 326–335, https://doi.org/10.1038/nature17041, 2016 5297586.
[75] N. Ferrara, Vascular endothelial growth factor: basic science and clinical progress, Endocr. Rev. 25 (2004) 581–611, https://doi.org/10.1210/ER.2003-0027.

[76] T. Cindrova-Davies, O. Spasic-Boskovic, E. Jauniaux, D.S. Charnock-Jones, G. J. Burton, Nuclear factor-κb, p38, and stress-activated protein kinase mitogen-activated protein kinase signaling pathways regulate proinflammatory cytokines and apoptosis in human placental explants in response to oxidative stress : effects of antioxidant vitamins, Am. J. Pathol. 170 (2007) 1511, https://doi.org/10.2353/AJPATH.2007.061035.
[77] K. Zhang, Integration of ER stress, oxidative stress and the inflammatory response in health and disease, Int. J. Clin. Exp. Med. 3 (2010), 33./pmc/articles/PMC2848304/. (Accessed 14 January 2024).
[78] B.R. Santos, J.M. dos A. Cordeiro, L.C. Santos, L. da S. Santana, A.E. de J. Nascimento, J.F. Silva, Kisspeptin suppresses inflammasome-NLRP3 activation and pyroptosis caused by hypothyroidism at the maternal-fetal interface of rats, Int. J. Mol. Sci. 24 (2023) 6820, https://doi.org/10.3390/ijms24076820.
[79] S. Moghadam-Kia, C.V. Oddis, R. Aggarwal, Approach to asymptomatic creatine kinase elevation, Cleve. Clin. J. Med. 83 (2016) 37, https://doi.org/10.3949/CCJM.83A.14120.
[80] S. Sharma, G. Godbole, D. Modi, Decidual control of trophoblast invasion, Am. J. Reprod. Immunol. 75 (2016) 341–350, https://doi.org/10.1111/AJI.12466.
[81] L.K. Akison, M.D. Nitert, V.L. Clifton, K.M. Moritz, D.G. Simmons, Review: alterations in placental glycogen deposition in complicated pregnancies: current preclinical and clinical evidence, Placenta 54 (2017) 52–58, https://doi.org/10.1016/J.PLACENTA.2017.01.114.
[82] Q. Zhou, C. Gensch, C. Keller, H. Schmitt, J. Esser, M. Moser, J.K. Liao, MnTBAP stimulates angiogenic functions in endothelial cells through mitofusin-1, Vascul. Pharmacol. 72 (2015) 163–171, https://doi.org/10.1016/J.VPH.2015.05.007.
[83] B.J. Moeller, Y. Cao, C.Y. Li, M.W. Dewhirst, Radiation activates HIF-1 to regulate vascular radiosensitivity in tumors: role of reoxygenation, free radicals, and stress granules, (n.d.).
[84] G.X. Rosario, T. Konno, M.J. Soares, Maternal hypoxia activates endovascular trophoblast cell invasion, Dev. Biol. 314 (2008) 362–375, https://doi.org/10.1016/j.ydbio.2007.12.007.
[85] Z.N. Rabbani, I. Spasojevic, X. Zhang, B.J. Moeller, S. Haberle, J. Vasquez-Vivar, M.W. Dewhirst, Z. Vujaskovic, I. Batinic-Haberle, Antiangiogenic action of redox-modulating Mn(III) meso-tetrakis(N-ethylpyridinium-2-yl)porphyrin, MnTE-2-PyP(5+), via suppression of oxidative stress in a mouse model of breast tumor, Free Radic. Biol. Med. 47 (2009) 992–1004, https://doi.org/10.1016/J.FREERADBIOMED.2009.07.001.
[86] I. Batinic-Haberle, A. Tovmasyan, I. Spasojevic, Mn Porphyrin-Based Redox-Active Drugs: Differential Effects as Cancer Therapeutics and Protectors of Normal Tissue against Oxidative Injury, vol. 29, 2018, pp. 1691–1724, https://doi.org/10.1089/ARS.2017.7453. Home.Liebertpub.Com/Ars.
[87] K. Watanabe, S. Shibuya, Y. Ozawa, H. Nojiri, N. Izuo, K. Yokote, T. Shimizu, Superoxide dismutase 1 loss disturbs intracellular redox signaling, resulting in global age-related pathological changes, BioMed Res. Int. 2014 (2014), https://doi.org/10.1155/2014/140165.
[88] S. Dey, A. Sidor, B. O'Rourke, Compartment-specific control of reactive oxygen species scavenging by antioxidant pathway enzymes, J. Biol. Chem. 291 (2016) 11185–11197, https://doi.org/10.1074/JBC.M116.726968.
[89] C.Y. Chen, C.P. Chen, K.H. Lin, Biological functions of thyroid hormone in placenta, Int. J. Mol. Sci. 16 (2015) 4161–4179, https://doi.org/10.3390/IJMS16024161, 2015, Vol. 16, Pages 4161-4179.
[90] Y. Zhao, D.W. Carroll, Y. You, L. Chaiswing, R. Wen, I. Batinic-Haberle, S. Bondada, Y. Liang, D.K. St Clair, A novel redox regulator, MnTnBuOE-2-PyP5+, enhances normal hematopoietic stem/progenitor cell function, Redox Biol. 12 (2017) 129–138, https://doi.org/10.1016/J.REDOX.2017.02.005.
[91] Y. Xu, D. Sun, C. Song, R. Wang, X. Dong, MnTMPyP inhibits paraquat-induced pulmonary epithelial-like cell injury by inhibiting oxidative stress, J. Toxicol. Sci. 43 (2018) 545–555, https://doi.org/10.2131/JTS.43.545.
[92] T. Kawakami, M. Yoshimi, Y. Kadota, M. Inoue, M. Sato, S. Suzuki, Prolonged endoplasmic reticulum stress alters placental morphology and causes low birth weight, Toxicol. Appl. Pharmacol. 275 (2014) 134–144, https://doi.org/10.1016/J.TAAP.2013.12.008.
[93] L. Du, F. He, L. Kuang, W. Tang, Y. Li, D. Chen, eNOS/iNOS and endoplasmic reticulum stress-induced apoptosis in the placentas of patients with preeclampsia, J. Hum. Hypertens. 311 (31) (2016) 49–55, https://doi.org/10.1038/jhh.2016.17, 2017.
[94] K.P. Robb, T. Cotechini, C. Allaire, A. Sperou, C.H. Graham, Inflammation-induced fetal growth restriction in rats is associated with increased placental HIF-1α accumulation, PLoS One 12 (2017) e0175805, https://doi.org/10.1371/JOURNAL.PONE.0175805.
[95] C. Hu, Y. Yang, M. Deng, L. Yang, G. Shu, Q. Jiang, S. Zhang, X. Li, Y. Yin, Y. Yin, C. Tan, C. Tan, G. Wu, Placentae for low birth weight piglets are vulnerable to oxidative stress, mitochondrial dysfunction, and impaired angiogenesis, Oxid. Med. Cell. Longev. 2020 (2020), https://doi.org/10.1155/2020/8715412.
[96] J.E. Thaxton, S. Sharma, Interleukin-10: a multi-faceted agent of pregnancy, Am. J. Reprod. Immunol. 63 (2010) 482, https://doi.org/10.1111/J.1600-0897.2010.00810.X.
[97] J.F. Silva, N.M. Ocarino, R. Serakides, J.F. Silva, N.M. Ocarino, R. Serakides, Spatiotemporal expression profile of proteases and immunological, angiogenic, hormonal and apoptotic mediators in rat placenta before and during intrauterine trophoblast migration, Reprod. Fertil. Dev. 29 (2017) 1774–1786, https://doi.org/10.1071/RD16280.
[98] A. Ahmed, C. Dunk, S. Ahmad, A. Khaliq, Regulation of placental vascular endothelial growth factor (VEGF) and placenta growth factor (PlGF) and soluble flt-1 by oxygen— a review, Placenta 21 (2000) S16–S24, https://doi.org/10.1053/PLAC.1999.0524.
[99] G. Tumurkhuu, N. Koide, J. Dagvadorj, F. Hassan, S. Islam, Y. Naiki, I. Mori, T. Yoshida, T. Yokochi, MnTBAP, a synthetic metalloporphyrin, inhibits production of tumor necrosis factor-α in lipopolysaccharide-stimulated RAW 264.7 macrophages cells via inhibiting oxidative stress-mediating p38 and SAPK/JNK signaling, FEMS Immunol. Med. Microbiol. 49 (2007) 304–311, https://doi.org/10.1111/J.1574-695X.2006.00203.X.
[100] H.L. Liang, G. Hilton, J. Mortensen, K. Regner, C.P. Johnson, V. Nilakantan, MnTMPyP, a cell-permeant SOD mimetic, reduces oxidative stress and apoptosis following renal ischemia-reperfusion, Am. J. Physiol. Renal Physiol. 296 (2008) F266–F276, https://doi.org/10.1152/AJPRENAL.90533.2008.
[101] P. Chatterjee, V.L. Chiasson, K.R. Bounds, B.M. Mitchell, Regulation of the anti-inflammatory cytokines interleukin-4 and interleukin-10 during pregnancy, Front. Immunol. 5 (2014) 1, https://doi.org/10.3389/FIMMU.2014.00253/BIBTEX, 1.
[102] J. Cao, Q. Peng, NLRP3 inhibitor tranilast attenuates gestational diabetes mellitus in a genetic mouse model, Drugs R 22 (2022) 105–112, https://doi.org/10.1007/S40268-022-00382-7/FIGURES/6.
[103] S. Corrêa-Silva, A.P. Alencar, J.B. Moreli, A.U. Borbely, L. de S. Lima, C. Scavone, D.C. Damasceno, M.V.C. Rudge, E. Bevilacqua, I.M.P. Calderon, Hyperglycemia induces inflammatory mediators in the human chorionic villous, Cytokine 111 (2018) 41–48, https://doi.org/10.1016/J.CYTO.2018.07.020.
[104] P. Gao, Y. Zha, X. Gong, F. Qiao, H. Liu, The role of maternal–foetal interface inflammation mediated by NLRP3 inflammasome in the pathogenesis of recurrent spontaneous abortion, Placenta 101 (2020) 221–229, https://doi.org/10.1016/J.PLACENTA.2020.09.067.
[105] N. Gomez-Lopez, K. Motomura, D. Miller, V. Garcia-Flores, J. Galaz, R. Romero, Inflammasomes: their role in normal and complicated pregnancies, J. Immunol. 203 (2019) 2757–2769, https://doi.org/10.4049/JIMMUNOL.1900901.
[106] K. Shirasuna, T. Karasawa, M. Takahashi, Role of the NLRP3 inflammasome in preeclampsia, Front. Endocrinol. 11 (2020) 503953, https://doi.org/10.3389/FENDO.2020.00080/BIBTEX.
[107] L.R. Villegas, D. Kluck, C. Field, R.E. Oberley-Deegan, C. Woods, M.E. Yeager, K. C. El Kasmi, R.C. Savani, R.P. Bowler, E. Nozik-Grayck, Superoxide Dismutase Mimetic, MnTE-2-PyP, Attenuates Chronic Hypoxia-Induced Pulmonary Hypertension, Pulmonary Vascular Remodeling, and Activation of the NALP3 Inflammasome, vol. 18, 2013, pp. 1753–1764, https://doi.org/10.1089/ARS.2012.4799. Home.Liebertpub.Com/Ars.
[108] B. Denkl, N. Cordasic, H. Huebner, C. Menendez-Castro, M. Schmidt, A. Mocker, J. Woelfle, A. Hartner, F.B. Fahlbusch, No evidence of the unfolded protein response in the placenta of two rodent models of preeclampsia and intrauterine growth restriction, Biol. Reprod. 105 (2021) 449–463, https://doi.org/10.1093/BIOLRE/IOAB087.
[109] W. Tong, E. Ganguly, R. Villalobos-Labra, A. Quon, F. Spaans, D.A. Giussani, S. T. Davidge, Sex-specific differences in the placental unfolded protein response in a rodent model of gestational hypoxia, Reprod. Sci. 1 (2022) 1–4, https://doi.org/10.1007/S43032-022-01157-W/FIGURES/2.
[110] J.M. dos Anjos Cordeiro, L.C. Santos, B.R. Santos, E.O. Santos, A.E. de J. Nascimento, G.J.C. de Freitas, J. de L. Singulani, D. de A. Santos, M.S.L. de Lavor, J.F. Silva, Redox profile and mediators of the unfolded protein response (UPR) in the placenta of rats during pregnancy, Reprod. Fertil. Dev. 35 (2023) 539–551, https://doi.org/10.1071/RD22123.